NOAA Technical Memorandum ERL SEL-63

VARIATIONS IN SOLAR UV SPECTRAL IRRADIANCE AND X-RAY FLUX

Richard F. Donnelly

Space Environment Laboratory
Boulder, Colorado
September 1982

noaa NATIONAL OCEANIC AND ATMOSPHERIC ADMINISTRATION / Environmental Research Laboratories

NOAA Technical Memorandum ERL SEL-63

VARIATIONS IN SOLAR UV SPECTRAL IRRADIANCE AND X-RAY FLUX

Richard F. Donnelly

Space Environment Laboratory
Boulder, Colorado
September 1982

UNITED STATES
DEPARTMENT OF COMMERCE

Malcolm Baldrige,
Secretary

NATIONAL OCEANIC AND
ATMOSPHERIC ADMINISTRATION

John V. Byrne,
Administrator

Environmental Research
Laboratories

George H. Ludwig
Director

NOTICE

Mention of a commercial company or product does not constitute an endorsement by NOAA Environmental Research Laboratories. Use for publicity or advertising purposes of information from this publication concerning proprietary products or the tests of such products is not authorized.

TABLE OF CONTENTS

VARIATIONS IN SOLAR UV SPECTRAL IRRADIANCE AND X-RAY FLUX

Richard F. Donnelly
NOAA/ERL/SEL
Boulder, Colorado 80303

ABSTRACT

Solar variations in the UV spectral irradiance are discussed with emphasis on the wavelengths important for producing or destroying ozone and heating the stratosphere. Short-term variations of days and weeks have now been well observed by the NIMBUS-7 and SME satellites. The size of the short-term variations at wavelengths longer than 160 nm are smaller than the 7% annual variation in incident flux produced by the orbital variations in the Sun-Earth distance. The percentage short-term variations are about twice as strong at the ozone production wavelengths as at the ozone destruction and stratospheric heating wavelengths. The short-term temporal variations are not simple sinusoids of the 27 day solar-rotation rate but include a much larger range of periods and also shifts in phase according to the location and apparent motion of active regions on the sun. Intermediate-term UV variations lasting a few months, associated with major rounds of solar activity, are discussed. They may account for some of the missing energy blocked by sunspots. The very important long-term and solar-cycle variations are the most poorly observed because of problems in satellite instrument degradation in space and difficulties in intercomparing measurements from different experiments. Long-term results are reviewed with emphasis on their limitations and speculation on long-term trends other than the 11 year sunspot cycle. Progress in modeling the solar UV flux temporal variations based on solar spatial data is reviewed with emphasis on the role of modeling in intercomparing isolated measurements and for providing better UV estimates for past times than indices like the 10.7 cm solar radio flux or sunspot number can provide.

RECENT REVIEWS

Solar UV radiation and its temporal variations have been recently reviewed by Heath (1980) and Simon (1981, 1982). The AE-E UV observations have been discussed by Hinteregger (1981). Simon's reviews have provided quantitative comparisons of UV measurements recorded at different times and grouped

according to their general level of activity. Simon pointed out the dilemma that some apparent discrepancies among measurements were roughly comparable to the expected magnitude of long-term UV temporal variations. For recent rocket-flight and balloon measurements, see Mount et al. (1980, 1981), Rottman (1981) and Simon et al. (1982a,b). Heath presented new observations from the NIMBUS-7 satellite of short-term UV variations and also evidence suggesting long-term secular UV variations. The present review emphasizes the recent NIMBUS-7 measurements and first results from the SME satellite. The limitations of solar indices for estimating the solar UV flux are discussed. Recent progress in modeling the solar UV flux based on solar spatial inhomogenieties measured by Ca II plage data is emphasized. The solar soft X-ray flux important to the upper mesosphere and D-region of the ionosphere is reviewed briefly.

INSTRUMENT DEGRADATION

Instruments that have measured solar UV spectral irradiance have degraded in the harsh environment of space. We do not have a good understanding of the degradation processes involved. Degradation in space causes the accuracy of the measurements to become poorer with time, usually by an unknown amount. Consequently, there is a cloud of uncertainty over past measurements, and observed variations are suspected of being caused by unknown instrumental drifts as much as by real solar flux variations.

Instrument designers have learned how to reduce the degradation by stowing certain optical surfaces except when they are required for a measurement. Also, the UV experiment on the recently launched SME satellite includes refer-

ence reflectance diffuser plates that are normally stowed except when they are deployed about once every two months in order to check the degradation of similar diffusers that are deployed daily for solar flux measurements (Rottman et al., 1982). The deduced degradation was less than 1%. The SUSIM instrument designed by NRL for use on shuttle flights and the future UARS satellites includes an entire second instrument for reference measurements as well as a deuterium lamp for in-flight calibrations (VanHoosier et al., 1981). The SBUV/2 instruments currently being built for NASA for future flights on NOAA satellites also include in-flight calibrations that include the diffuser in the calibration. The combination of short-term measurements from rocket flights and future shuttle measurements should provide calibration checks for longer-term satellite measurements. Consequently, there is hope that we will emerge from the cloud of uncertainty in solar UV irradiance measurements to satisfactorily measure long-term solar UV variations. However, we should proceed with caution, seeking concurrent corroboration of observed variations and a full physical understanding of the variations in terms of the spatial distribution of regions of enhanced emission on the solar disk and their altitude dependence in the sun.

ATMOSPHERIC IMPORTANCE

Figure 1 illustrates the interaction of the solar UV flux with the atmosphere. The solar UV flux intensity generally decreases with decreasing wavelength at wavelengths longer than 400 nm. This decrease steepens below the Al I absorption edge in the solar spectrum near 210 nm and then levels out on the average at wavelength below 120 nm, but with highly irregular variations with

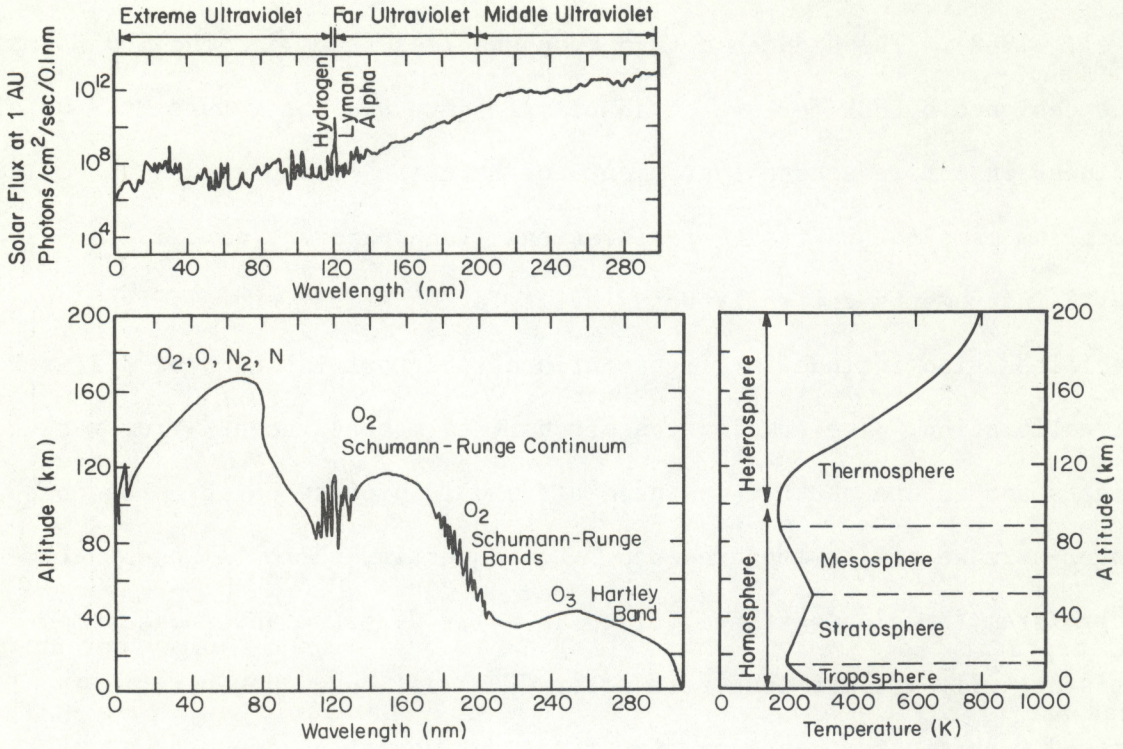

Figure 1.--The relation between solar UV radiation, the altitude dependence of UV absorption and the layers of the atmosphere based on the altitude dependence of temperature (Lean, private communication, 1981).

wavelength over wavelength ranges of a few nm. When viewed with finer wavelength resolution, the solar spectrum includes numerous absorption lines longward of about 150 nm and numerous emission lines shortward of about 182 nm. The known variability generally increases with decreasing wavelength from the order of 0.1% at optical wavelengths, to about 1% in the 200-300 nm range, to 10's% in the 10-160 nm range to a few orders of magnitude (100X-1000X) in the soft X-rays (~ 1 nm). This trend is not perfectly monotonic with wavelength but is a more systematic function of the solar temperature of the UV source regions. The intensity of the Lyman α line near 122 nm exceeds the intensity of all the solar radiation at shorter wavelengths.

The lower left hand graph in Figure 1 shows the altitude where the optical depth of the solar radiation at UV wavelengths equals unity for an overhead sun, i.e., the altitude at which the solar radiation has been attenuated to 1/e of its incident value. Much of the solar radiation at a given wavelength is absorbed in the Earth's atmosphere near the altitude of unit optical depth. The graph on the right side of Figure 1 indicates the atmospheric layers and temperature as a function of altitude. Clearly the UV radiation does not have a direct major effect on the troposphere because the UV radiation is absorbed at higher altitudes. The stratosphere is strongly influenced by solar UV radiation and any UV influence on climate therefore requires strong coupling effects from the stratosphere to the troposphere. The 200-300 nm UV radiation that penetrates to the stratosphere includes the 220-285 nm range which is primarily absorbed by ozone (O_3) and is the major source of stratospheric heating and ozone photodissociation. On the other hand, radiation below 242 nm can photodissociate molecular oxygen (O_2) and the resultant oxygen

atoms can recombine with molecular oxygen to produce ozone. This is particularly important in the Schumann-Runge bands where O_2 dominates the UV absorption (~ 175-200 nm). The UV radiation that penetrates deepest into the stratosphere is in the range ~ 195-215 nm and is sometimes called the window region. In later discussions of UV variability, we will refer to the 175-205 nm range as being predominately related to ozone production and the 205-295 nm as being the predominant source of direct solar heating and ozone photodissociation in the stratosphere. The 175-300 nm solar UV flux variations are of primary interest for research into a possible connection between solar activity and climate via solar control of the stratosphere and coupling from the stratosphere to the troposphere.

Note that the strong Lyman α solar emission line is at a wavelength that corresponds to a local minimum in the O_2 absorption spectrum so that it penetrates into the mesosphere where it photodissociates water vapor, which contributes to the destruction of ozone at about 70 km altitude. Because of the importance of 300-330 nm solar radiation for ground-based monitoring of atmospheric ozone, it is also important to determine whether solar flux variations occur at these wavelengths. Temporal variations of Lyman α and 300-330 nm radiation are second in importance for UV-climate research.

Radiation in the 120-175 nm range contributes to heating the thermosphere and the production of atomic oxygen. The EUV flux below 103 nm contributes to the E and F region ionization. During high levels of solar activity, the highly variable X-ray flux below 1 nm (together with cosmic rays and Lyman α) contributes to the D-region ionization at the top of the mesosphere. These radiations vary much more than the solar UV flux but they directly affect

atmospheric regions further removed from the troposphere and would require some complicated trigger-coupling mechanisms in order to influence climate. Because these radiations vary by larger percentages than the UV flux longward of 175 nm, they are useful for studying variations in the solar atmosphere that are related to changes in the solar atmosphere at lower heights where the variations longward of 175 nm originate. These radiations are third in importance in research of solar UV variations and their possible effects on climate.

SHORT-TERM VARIATIONS

Short-term variations of UV flux on the order of days and weeks, caused by the combined effects of active region evolution (birth, growth, peak and decay) and solar rotation, have been known to exist for more than a decade (Heath, 1973, Hinteregger et al., 1977). Most climatologists think in terms of much longer time scales than weeks, but these short-term variations are very important because of the following: (1) Recent measurements of short-term variations make them the first solar UV variations that are accurately observed-free from the ominous cloud of doubt caused by instrument degradation. (2) Research of their stratospheric effects can now proceed. (Observations of concurrent O_3 variations in the upper stratosphere in phase with the UV variations have been reported by Heath, 1982.) (3) Measurements of the short-term variations fairly well determine the contribution of plages to the solar-cycle UV variations. (4) To interpret long-term series of rocket and shuttle measurements, in order to measure long-term trends, we must accurately determine the short-term variations (equivalent to noise for the long-term trends) at the time of each measurement in the series.

Figure 2 shows an example of UV measurements by the Solar Backscatter Ultraviolet (SBUV) Experiment on the NIMBUS-7 satellite. Note the short-term variations over several weeks. The amplitude is highest at the shortest wavelength shown (~ 4%).

Below the 280 nm curve in Figure 2, the magnitude is indicated for the annual variation in all solar electromagnetic flux, independent of wavelength, that is incident at the top of the Earth's atmosphere. This variation is caused by the annual variations in the Sun-Earth distance. The circle denotes the average value, the top bar denotes the maximum value relative to the average and the bottom bar denotes the minimum. The ratio of maximum to minimum flux due to the annual Sun-Earth distance variation exceeds unity by about 6.9%. The peak in flux due to this annual sinusoidal effect occurs in early January, the minimum in early July, and the crossing of the average values in early April and October. These dates currently lag the solstices and equinoxes by about two weeks. We will use this precisely known annual variation as a gauge in discussing the importance of the magnitude of other observed variations. The UV flux in each figure in this paper has been corrected to the value at a constant distance of 1 AU from the sun, i.e., the annual variation for fluxes at Earth due to the Sun-Earth distance variation has been removed.

In Figure 2, the short-term variations are comparable but a little smaller in magnitude than the annual variation. Note also the long-term downward trend in the UV data that is large at 205 nm and weak at 182 and 280 nm. Much of this trend has recently been determined to be caused by a wavelength-dependent instrument degradation and is currently being corrected. But this effect

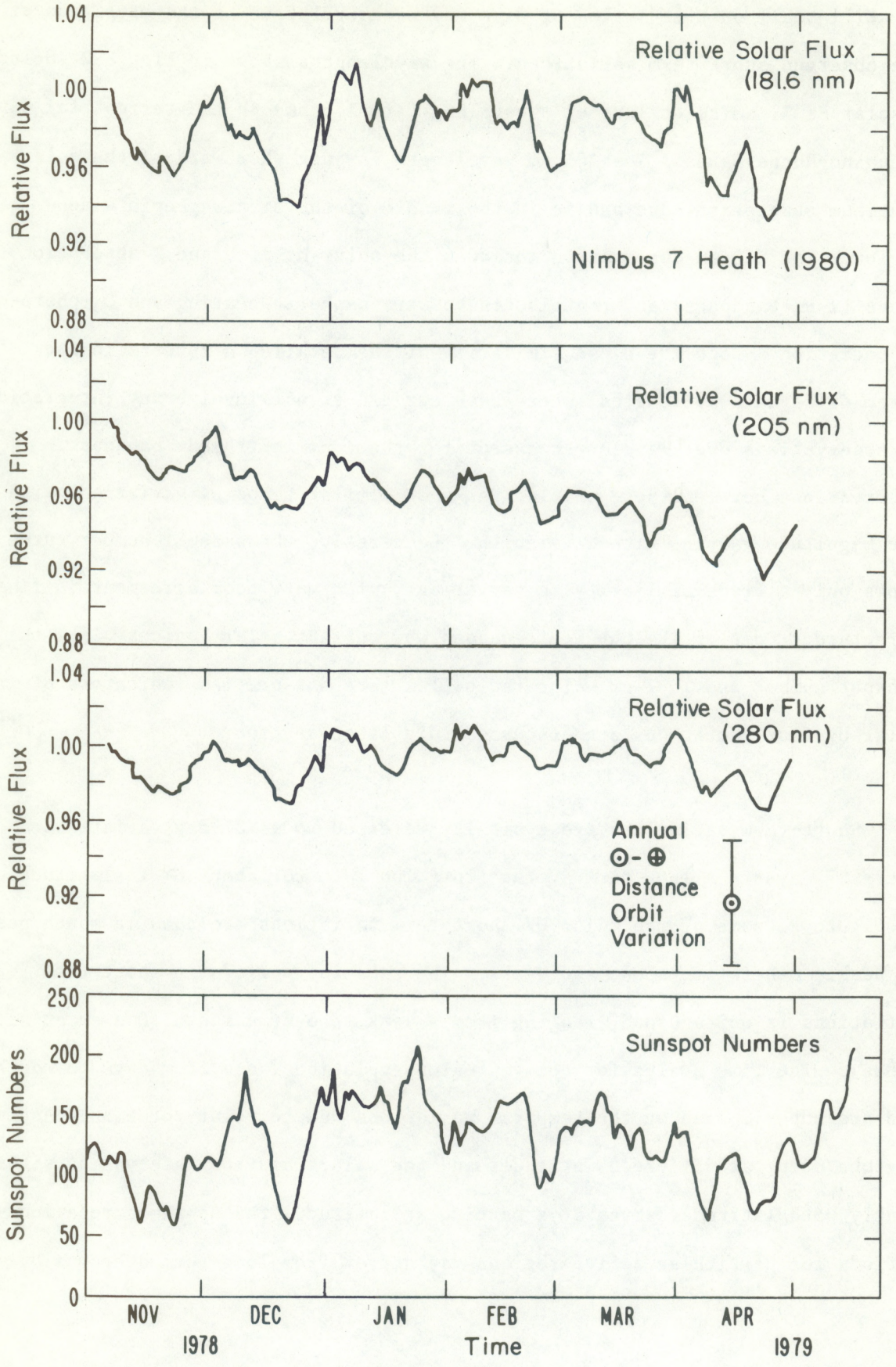

Figure 2.--NIMBUS-7 measurements of short-term variations at UV wavelengths of stratospheric influence.

is still small on time scales of days and weeks relative to the magnitude of the observed short-term variations. The wavelengths shown in Figure 2 include a solar Si II emission line at a wavelength (181.6 nm) in the terrestrial O_2 Schumann-Runge bands. The 205 nm wavelength is just shortward of the solar aluminum absorption edge and is in the middle of the stratospheric window region. The 280 nm observation includes the solar Mg II H and K absorption lines (1 nm bandpass) and contributes to stratospheric heating and O_3 photodissociation. Note the close similarity of the detailed structure in the three different wavelengths, where each curve does not involve any integration of observations over wavelength except for the 1 nm instrument bandpass. Observations between these wavelengths show similar temporal variations with the magnitude varying with wavelength. Conversely, the sunspot number curve shows only a crude similarity in variations, with very poor agreement in fine structure. Some of the physical reasons why current solar indices, like the sunspot number and 10.7 cm solar radio flux, are not precise indicators of solar UV flux variations are discussed in a later section.

Short-term variations are typically referred to as 27-day variations where 27 days is a long-term average rotation rate for about 8° in latitude. In Figure 2, some of the major UV short-term variations are about a month peak to peak. Others are about two weeks. The range of periods in short-term variations is quite broad, ranging from a week to over a month (Bouwer et al., 1982a). The time scales for active region evolution range from days to months and are superimposed on the temporal variations due to solar rotation. Active regions occur at different latitudes and the solar rotation rate varies significantly with latitude. Even at a particular latitude, the apparent rotation periods for particular active regions may differ from long-term averages by

several days. Bouwer et al. (1982a) have found a variety of short-term periods in X-ray and UV data during different "epochs" of solar activity. Periods of the order of 13 days are caused by clusters of active regions about 180° apart in solar longitude that cause two peaks in emission per rotation. The rise of new dominant groups of active regions at new solar longitudes, or the decay of older dominant regions, causes phase shifts in UV flux variations at particular periods. Clearly, short-term variations are not simple periodic variations as might be inferred by the label "27-day variations." Use of this over-simplified label should be discontinued. The variations in Figure 2 occurred during high levels of solar activity. During the local minima in these short-term UV variations, there are still quite a few active regions (plages) on the visible sun. The variations observed are caused by both the temporal evolution of plages (birth, growth, peak and decay) and the solar rotation of a nonuniform distribution of plages with longitude, and not simply by the presence and then complete disappearance of all active regions from the solar disk.

Figure 3 illustrates the first results from the Solar Mesosphere Explorer Satellite (SME) in the UV wavelengths corresponding to the O_2 Schumann-Runge bands, important for the stratosphere and mesophere, the Lyman α line of mesospheric importance, and the UV wavelengths corresponding to the Schumann-Runge continuum that is important for the lower thermosphere. The average solar rotation variations in the 175-190 nm and 130-175 nm ranges are about 8%, which is a little larger than the size of the annual variation produced by the Earth's orbit ellipticity around the sun. The Lyman α variation is much larger, an average of about 50%, and a maximum to minimum ratio of almost 100%. Note that the short-term variations increase both by achieving deeper valleys as well as higher peaks in the mid-November through December period than in

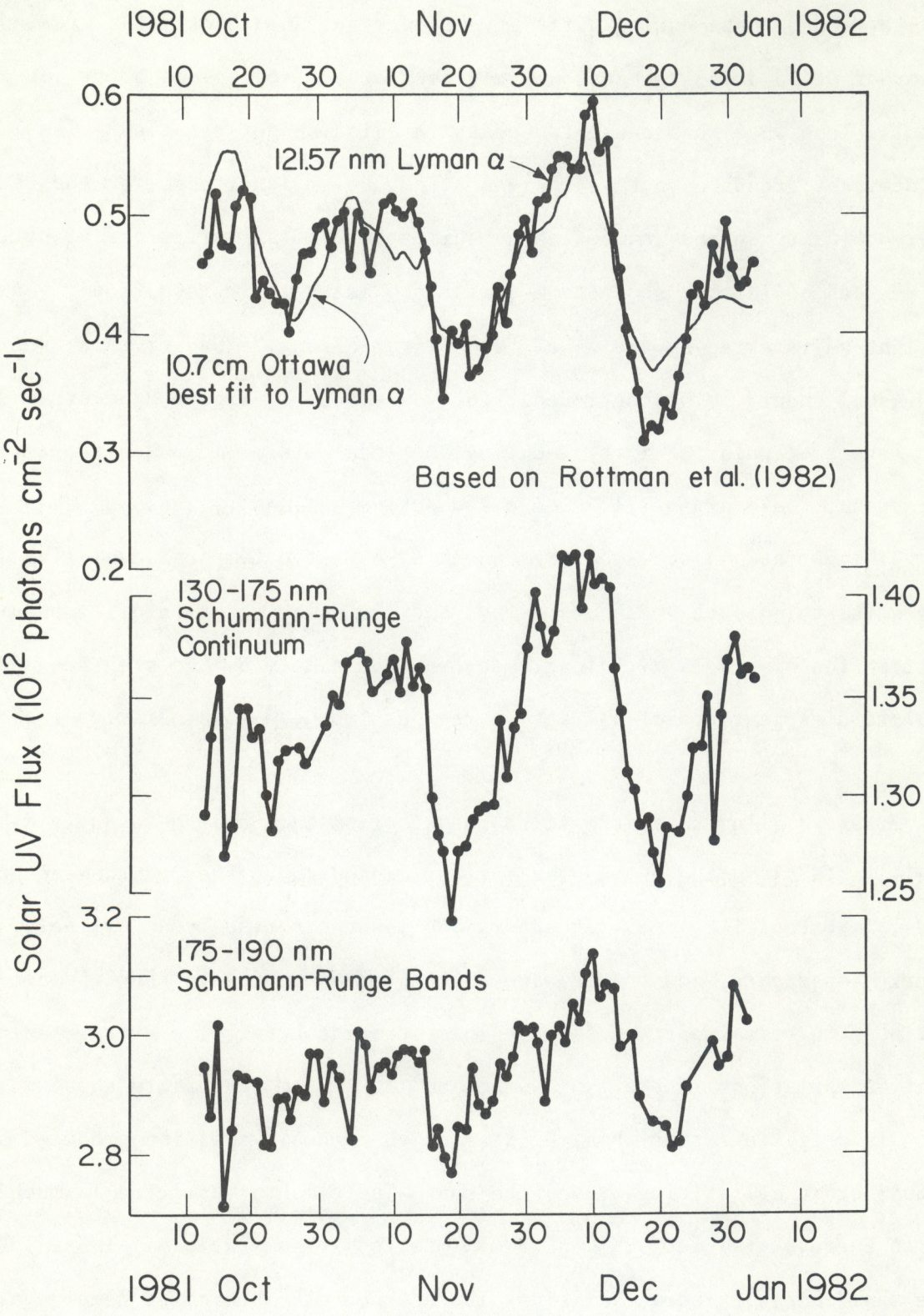

Figure 3.--SME measurements of short-term UV variations.

the October period. The maps of solar activity in Solar Geophysical Data show in October small variations in plage area with solar longitude. Conversely, in the latter half of November and in December, the activity developed primarily in one hemisphere in longitude with extensive bright plages while the other hemisphere consisted of fainter scattered plages. The 10.7 cm radio flux curve in Figure 3 was the best linear regression fit for the whole data set shown (Rottman et al., 1982). It shows a similar variation but does not agree in detail with the observations. These SME measurements of short-term variations in the Schumann-Runge-band wavelengths phenomenologically corroborate the NIMBUS-7 observations in that both experiments observe the same type of variation with similar intensities. Direct comparison of concurrent measurements has not yet occurred, but would be an excellent opportunity to achieve concurrent corroborating measurements.

Figure 4 compares preliminary total solar irradiance S(t) data with concurrent UV data from Heath's SBUV experiment and the NOAA solar X-ray monitoring measurements from the GOES-2 satellite. Note that the variations in S (primarily photospheric) are of the order of tenths of percent, the UV variations (lower chromosphere and upper photosphere) are a few percent, and the X-ray variations (corona) are an order of magnitude.

The X-ray data used in Figure 4 is an estimate of the midday nonflare background flux and exhibits much less variability than the daily mean X-ray flux that is highly influenced by solar flares (Bouwer et al, 1982). Hickey (1982, private communication) has reported that special corrections are now being made to the S(t) data such that the major dip of August 1979 will not be as deep as indicated by the preliminary engineering data. However, it will

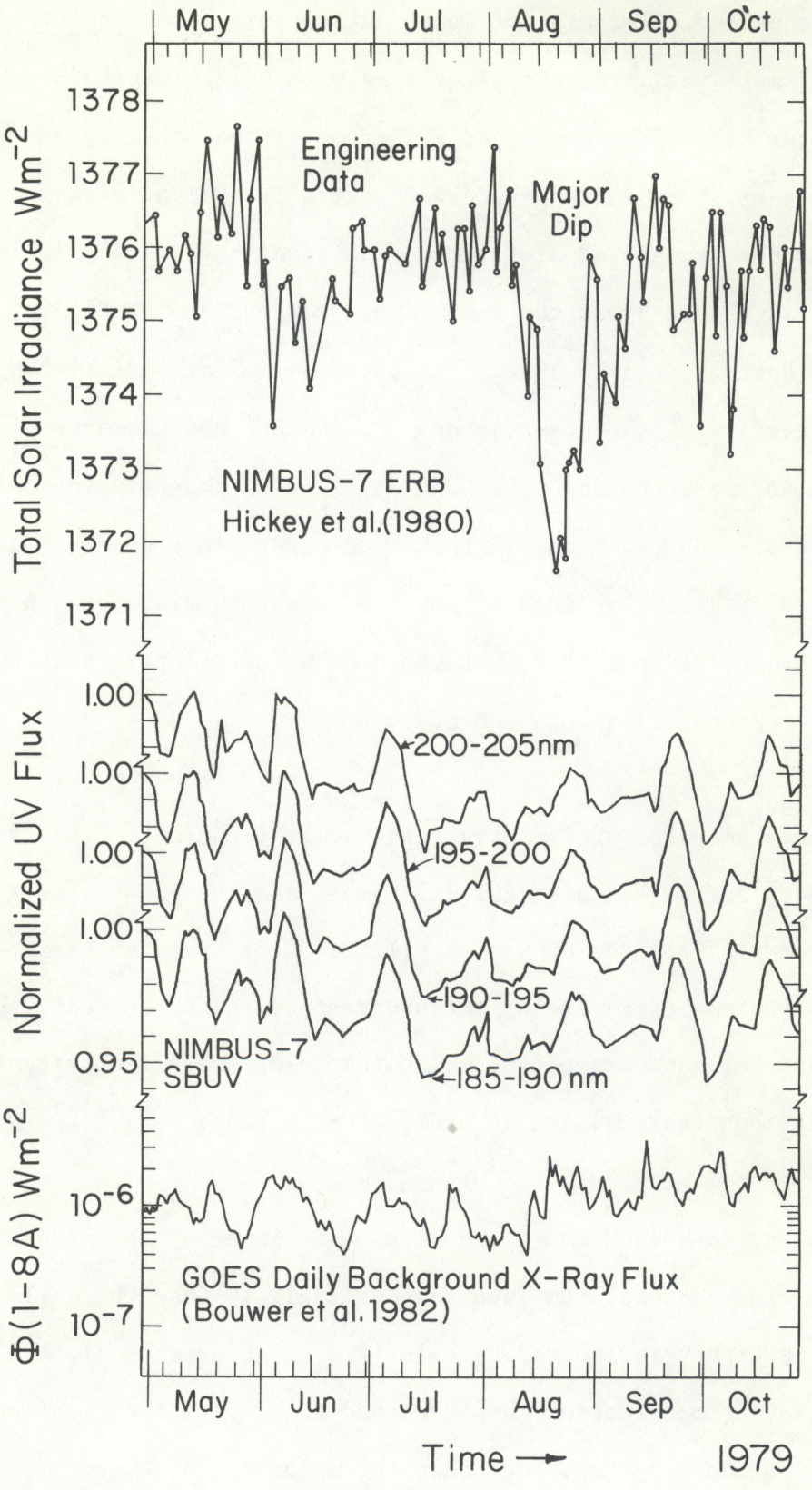

Figure 4.--Short-term variations are different for total solar irradiance, UV and X-ray flux (Donnelly et al., 1982).

still be one of the major dips caused by the net darkening effect of large sunspots clustered in a small CMD range crossing the center of the solar disk. The modeling of Hoyt and Eddy (1982) also indicates that the August decrease is one of the major dips in S. At the same time as the major dip caused by large sunspots near the center of the disk, the UV shows only a minor enhancement caused by the plages associated with the same active regions. Similarly, the coronal X-rays do show an enhancement but not an outstanding one at the time of the major dip in S. In conclusion, the short-term variations in S, UV and X-rays differ significantly.

Note that in May and early June, the major peaks in the UV data are about every thirteen days. This results from groups of plages, located roughly 180° apart, rotating into and out of view at Earth. Note also that the related peaks of April 30 and May 26 form a series where the intensity and area of the plages involved are decaying and are very weak near June 22. On the other hand, the series of quasi-periodic peaks of May 13, June 9, July 7, July 31, August 25 and September 22 is long lasting because of the emergence of new activity near the same solar longitudes with a small shift in phase or longitude during the small double peaked enhancement near the end of July, 1979. Figure 5 shows in greater detail the double peaked enhancement of late July and early August where the first peak appears to be related to the following portion of the long series of peaks. The squares in Figure 5 denote the intensity and time of the daily average of SBUV measurements of solar UV flux, where measurements were not made on some days. Most of the peaks in the 175-200 nm range caused by active regions grouped in a small range of solar longitude have half-maximum widths of about eight days, wider at shorter wavelengths, which is the case in the UV enhancement of August 20 to September 2

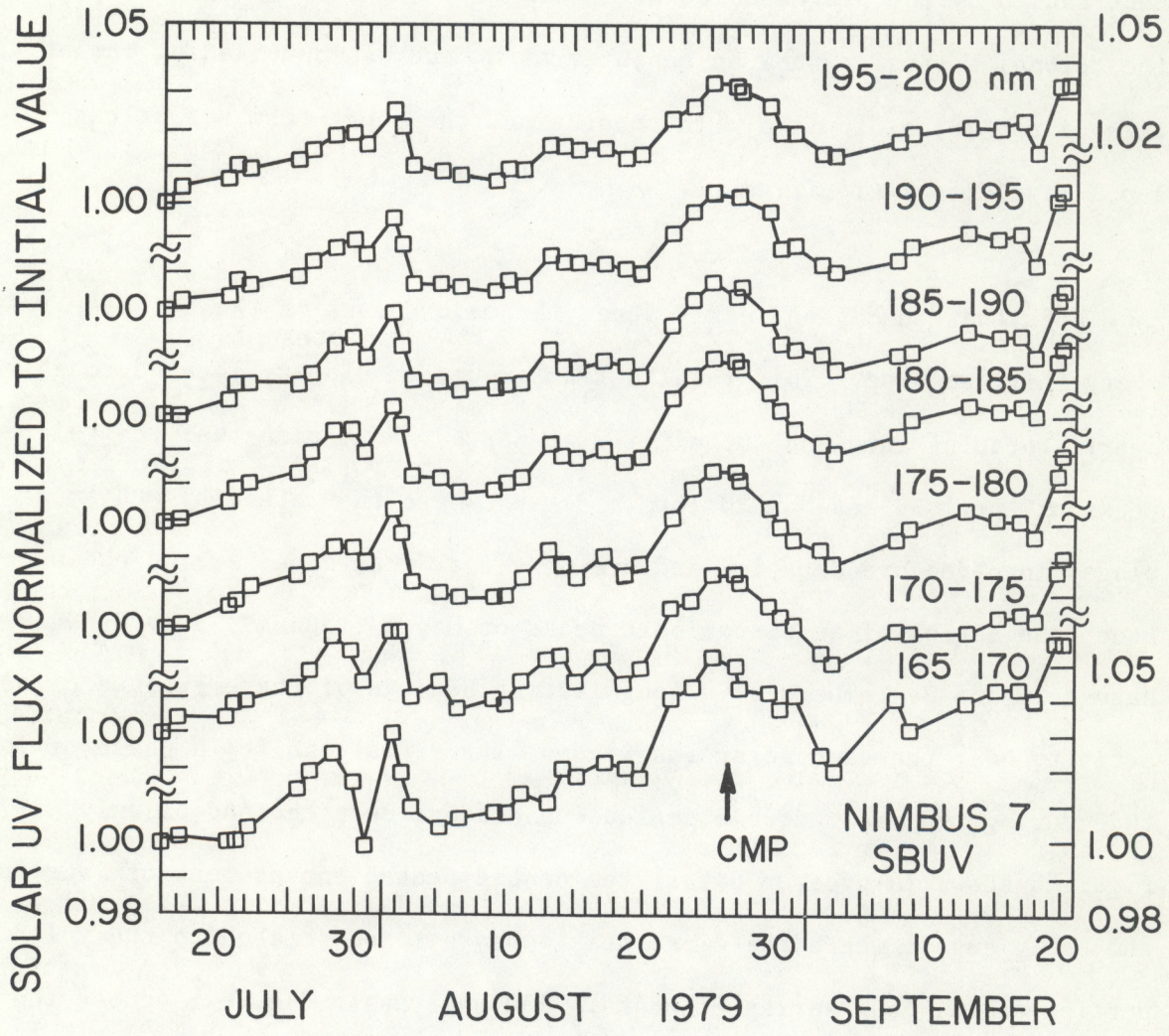

Figure 5.--NIMBUS-7 measurements of short-term UV variations with an enlarged time scale (Donnelly et al., 1982).

in Figure 5. The peak on August 25 occurred just before the central meridian passage (marked CMP in Figure 5) of the major active regions involved.

Figure 6 shows the spectrum of the ratio of the flux at the peak to that at the minimum for short term variations observed with a 1 nm bandpass. This figure is based on an average over three short-term variations comparing the peaks of December 2, 1978, January 2 and February 5, 1979, with the minima of December 21, 1978, January 18 and February 27, 1979 (Heath, 1980, Park and Heath, 1981). See Figure 2. These are slightly larger peaks than the average for Figures 2 and 4 but smaller than the variations of November-December, 1981, in Figure 3. In the 175-205 nm range that promotes production of ozone in the stratosphere, the short-term variations in Figure 6 are a little more than half the annual variations caused by the Earth's orbit ellipticity from July (bottom bar in Figure 6) to January (top bar). The stratospheric heating and ozone photodissociation wavelengths 205-300 nm vary by about half the 175-205 nm radiation and by about a fourth the annual orbital variation. The main solar physical features in Figure 6 are the aluminum (Al I) absorption edge just below 210 nm and the magnesium absorption continuum in the 210-250 nm range. Consequently, variations in the solar aluminum absorption dominate the short-term UV-induced changes in ozone production while concurrent changes in the solar magnesium absorption dominate the UV-induced changes in stratospheric heating and ozone photodissociation. Other prominent solar features in Figure 6 are the Mg II H and K lines at 280 nm (see also Figure 2) and the Mg I line at 285 nm. Numerous other lines of neutral and singly-ionized Mg, Ca, Fe, Al and Si are evident in the spectra (Heath and Park, 1982).

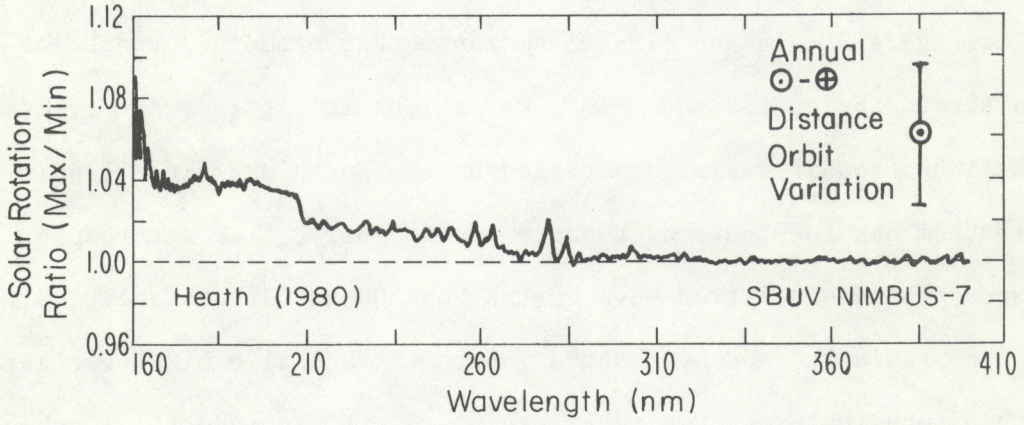

Figure 6.--Spectra of short-term UV variations.

The results on short-term variations presented in Figures 2-6 involve a combination of two types of variations, namely the temporal evolution of active regions (birth, growth, peak and decay) and the effects of solar rotation, including the foreshortening of optically-thick plage areas at large central meridian distances (CMD) and occultation effects at the edge of the visible solar disk, the solar limb. Measurements with spatial resolution are required to separate these two types of temporal variations. The spectra in Figure 6 should be predominantly due to solar-rotation (CMD) effects. The average spectrum of changes due entirely to temporal evolutions probably is quite similar in spectral shape to Figure 6, but spectra during the rapid growth of regions or late in their decay phase might differ slightly.

Figure 7 illustrates the variation of active-region radiation for several solar radiations as a function of CMD, where 0° is at the solar meridian that passes through the center of solar disk observed at Earth and on the average 90° is at the limb. The decrease in the photospheric total solar irradiance by active regions with large sunspots is illustrated by the curve for sunspot darkening minus faculae brightening, which is based on a model by Schatten et al. (1982) evaluated for the relative strength of faculae indicated by Hoyt and Eddy (1982). The UV plage brightening curve is based on a model by Lean et al. (1982), which is discussed further in the section on modeling. The soft X-ray curve beyond 83° and 10 cm radio curve are based on averages over many active regions in order to average out the temporal variations of individual active regions (Donnelly, 1982; Donnelly et al., 1982). The radio flux is optically thick and is emitted from above the chromosphere so that part of the coronal radio emission can still be observed when the chromospheric plages are beyond the solar limb. The X-ray emission is entirely from the coronal

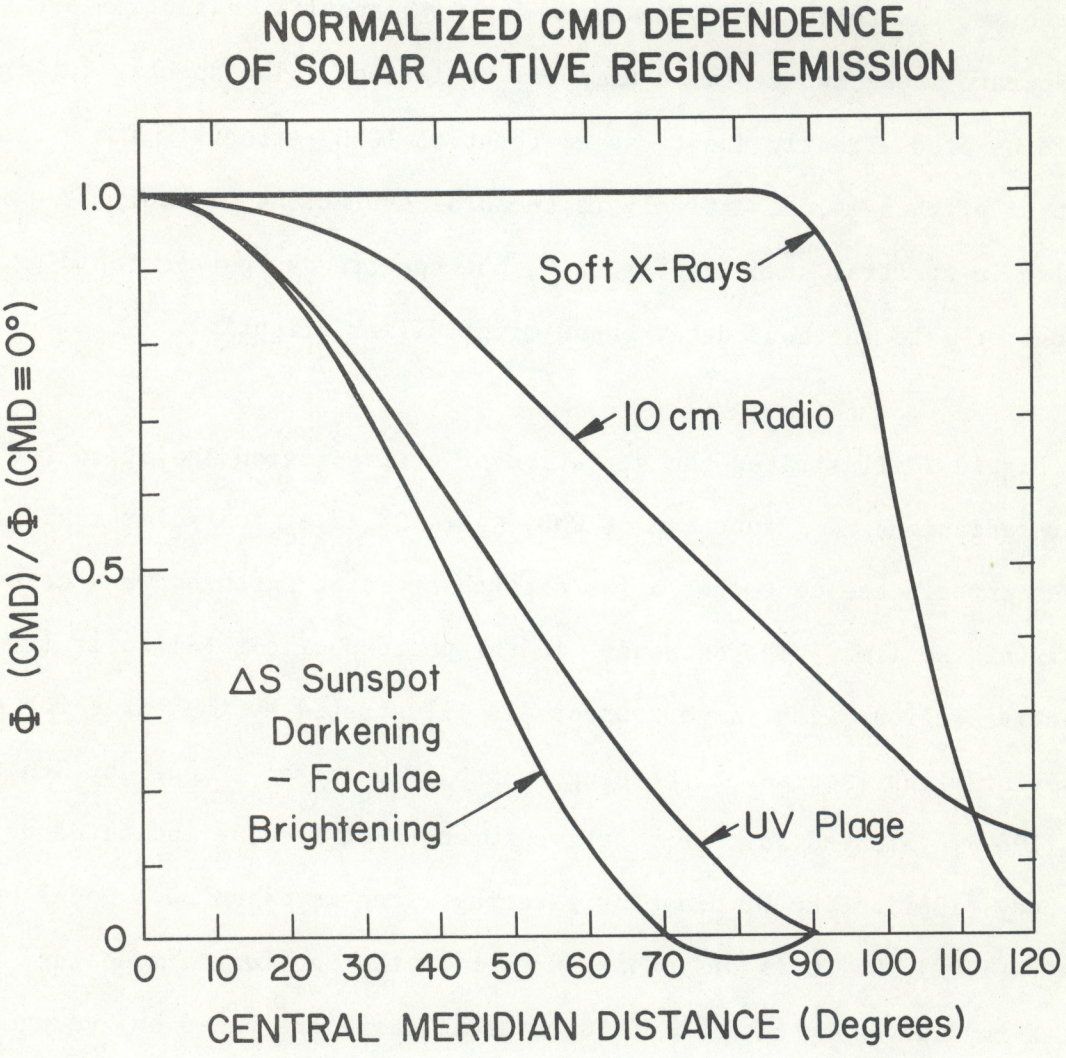

Figure 7.--Average CMD dependences of total solar irradiance, UV, 10 cm radio flux and soft X-rays (Donnelly et al., 1982).

portion of active regions and does not vary greatly with solar rotation until occultation effects occur for active regions at and beyond the limb. We do not have an appropriate curve for the sunspot number sensitivity to CMD, but expect it would be quite flat in the 0-70° range, dropping in the 70-80° range slightly and then dropping sharply to zero at 90°+, where the drop before 90° is caused by difficulties in seeing small sunspots near the limb.

For a typical synodic solar rotation rate of about 13.3° CMD per day, the temporal half-width would be about six days for darkening from a sunspot, about seven days for UV plage brightening (greater for wavelength shorter than 180 nm), eleven days for the 10 cm active region enhancement and about fifteen days for the corona soft X-ray emission of an active region. The half-width for sunspot number would probably be about twelve days. For an active region, or group of regions extended in CMD or solar longitude, the above half-widths would be correspondingly greater (~ 1 day per 13.3° CMD length). The half-widths evident in Figures 4 and 5 are consistent with the UV curve in Figure 7. Because the UV half-width is only about seven days and the typical rotation rate is about four times longer, strong enhancements with periods near 13 days can occur in the UV when strong groups of regions are located about 180° apart. (See the paper by Ebel and Schwister in this proceedings.) For such regions, the amplitude of the 13-day periodicity will be weaker in the 10.7 cm radio flux, and the sunspot number R_z. Because of their broader half-widths the soft X-ray flux can be at a maximum when the two groups of regions are at the East and West solar limbs, and at a minimum of about a factor of two lower than the maximum when one of the groups of regions is at the center of the disk, i.e., out of phase with the 13-day UV variation. This occurred in May, 1979, in Figure 4.

INTERMEDIATE-TERM VARIATIONS

Heath (1982) presented NIMBUS-7 observations showing an approximately semiannual variation in the 300-400 nm range as well as in the 160-300 nm range, unlike the short-term variations (and their associated solar cycle variations) in Figure 6. The largest of these intermediate enhancements occurs near the maximum of solar cycle 21, peaking in October-December, 1979, with a minimum to maximum enhancement of about 3% in the 300-400 nm range and about 6% at 170 nm. This particular peak may involve other processes compared to the other quasi-semiannual peaks that are an average of about 1% in peak amplitude in the 300-400 nm range. At wavelengths longer than 300 nm, these enhancements appear to be devoid of any solar rotation-modulation, so if they are real, they involve global solar enhancements. The peaks of the observed quasi-semiannual variations occurred at the end of November, 1978, early May and mid-November, 1979, May and December, 1980, May and after October (end of data shown) 1981, with minima near February and August in 1979-1981.

One suggestion was that these semiannual variations may be related to the semiannual variation in the amount of the solar polar regions that are visible because of the tilt of the solar axis of rotation with respect to the plane of the Earth's orbit around the sun, the ecliptic plane. The solar polar regions usually contain coronal holes, regions of reduced coronal emission. However, it is not known whether these regions are weaker in 170-400 nm emission. More important, as the northern polar region becomes more visible, the southern polar region becomes less visible, and the net change in polar regions in percent of the solar disk viewed at Earth, for example above 60° latitude, is negligible. Therefore, the semiannual variations in the view of solar polar regions at Earth cannot produce full-disk UV variations of the order of 1%.

According to Smith and Gottlieb (1974), the UV radiation at wavelengths shortward of 400 nm constitutes approximately 7.7% of the total solar irradiance (S). Therefore a 1% enhancement in the UV should correspond to at least 0.08% variation in S, and the 3% for the largest UV peak to about 0.2% in S, which is large enough to be observed in the NIMBUS-7 measurements of S (and the SMM measurements after their commencement of observations in February, 1980). On the other hand, measurements of S(t) are dominated by short-term variations of comparable magnitude that are primarily related to sunspot darkening. The latter may mask the presence in S(t) of semiannual variations related to the solar UV variations. However, considering that the UV spectrum of the semiannual variation probably does not fall sharply to zero with increasing wavelength longward of 400 nm, which would cause the effects on S(t) to exceed the above estimates, then recent concurrent S(t) measurements suggest (but do not prove) the semiannual variations (1979-1981) reported by Heath (1982) may not be real but may be due to unknown instrumentation drifts with wavelength characteristics different from the known drifts.

Willson (1982) has pointed out a 171-day period in projected sunspot area and 10.7 cm solar radio flux during 1980 with a minimum on August 12, 1980. The average period of Heath's quasi-semiannual UV variation in 1979-1981 was 5.7 months or about 171 days with an amplitude minimum in August, 1980. Furthermore, the model results discussed later suggest the presence of about four peaks in UV flux due to major rounds of activity in 1979 and 1980. Consequently, Heath's quasi-semiannual UV variations may be real and may result from a sequence of major rounds of solar activity. Heath (1982) has suggested that these UV enhancements may be some of the "missing" solar energy blocked by sunspots.

In conclusion, quasi-semiannual UV variations have been observed by Heath (1982). The largest such enhancement had an amplitude of about 3% in the 300-400 nm range with no detected solar-rotation modulation and occurred near the peak of solar cycle 21. Corroborating measurements of this observed phenomenon are needed to verify that it is not caused by an unknown instrumental drift.

SOLAR CYCLE VARIATIONS

The measurement results for variations over the solar cycle have recently been reviewed by Heath (1980) and Simon (1981). In the important 175-205 and 205-295 nm bands, the solar cycle variations have not yet been well measured. Existing measurements are plagued by apparent discrepancies among the measurements (Simon, 1981). We expect the spectrum of the solar cycle variation caused by the build-up of active regions to be similar in shape to the results in Figure 6 but larger in amplitude. The possibility of real semiannual variations in the 300-400 nm range discussed above also raises the question whether solar cycle variations of the order of one percent may also occur at wavelengths longer than 300 nm (other than those wavelengths dominated by chromospheric lines like Ca II H and K that are already known to vary).

Lean (1982, private communication) has estimated the solar cycle variation of UV flux based NIMBUS-7 data like that in Figure 6. Ca K plage variations corresponding to strong UV solar rotation variations were used, together with the plage build-up from sunspot minimum to sunspot maximum, to estimate the corresponding UV build-up. The resultant ratio of UV flux at the maximum

of solar cycle 21 to solar minimum caused by plage build-up was a little over 6% at 175 nm, decreasing to about 5% at 205 nm. The Si II lines near 180 nm rose to about 10% variation for a 1 nm bandpass with a spectral shape like that in Figure 6. The combined Mg II H and K lines at 280 nm were estimated to be enhanced by 4%, and there was about a 2% enhancement in the 210-270 nm range. These estimates probably underestimate the solar cycle variation because the solar activity accounted for in plages does not include numerous small plages (plagettes, Brueckner of Brueckner et al., 1976). Nor does it include the remnants of old active regions that are scattered among the chromospheric network and called the active-network. Lean's estimate that includes an active-network and plagette term as well as the major plages gives a spectra shape like that in Figure 6 except the enhancement magnitude is about 32% at 175 nm, 27% at 205 nm, 45% in the Si II lines near 180 nm, 12% at 210 nm, 10% at 260 nm, and 21% at the Mg II H and K lines near 280 nm. This implies that the effect of including plagettes and the active network is quite large. Clearly there is a need for accurate measurements to verify the current estimates.

Discrepancies among measurements of the Lyman α line are illustrated in Figure 8. Estimated error bars have not been included and in some cases are quite large. On the other hand, we would like to know the intensity of Lyman α flux variations over a solar cycle to an accuracy of about 5%, which is clearly beyond the recent state-of-the-art. The jump in the satellite data in December 1978 is surely not real. There were no sudden jumps in other solar activity parameters or solar spatial structure at that time. In general the satellite data in 1978 are higher than during the sunspot maximum of solar cycle 20 in 1969. This may be due to the particular "plausibility" argument

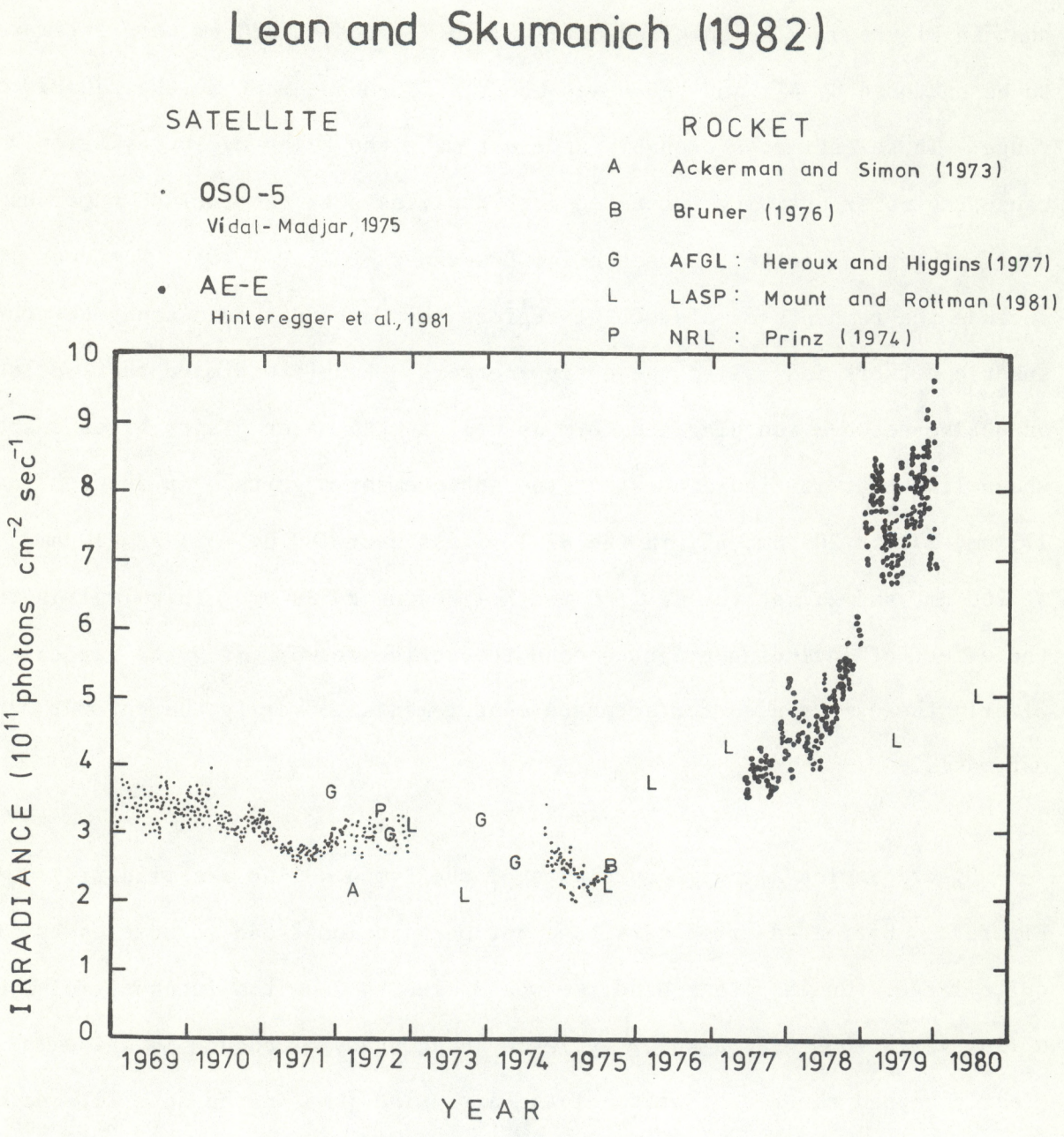

Figure 8.--Solar cycle variations of Lyman α measurements.

used to estimate the magnitude of the satellite intensities relative to an earlier rocket flight measurement (Lean and Skumanich, 1982). Note also that the rocket-flight measurement of 1979, near the maximum of solar-cycle 21, has about the same intensity as the 1977 measurement just after the end of the sunspot minimum phase and during the initial small rise of cycle 21. The solar cycle variation of Lyman α reported by Vidal-Madjar (1977) and Vidal-Madjar and Phissamay (1980) of about a factor of two enhancement is still the best estimate of the Lyman α variation over a sunspot cycle. In a later section, current and future measurements are discussed. Clearly, improvements are needed. Solar cycle variations are discussed further in the section on modeling the solar UV spectral irradiance.

There is a tendency for solar radiation variations to be assumed to consist of 27-day variations and the solar cycle variation. The short-term variations have been shown to include time scales from days through weeks. Quasi semiannual variations have been observed. In the next sections secular and long-term variations are discussed briefly. We must not neglect the possibility of UV variations on time scales other than the 27-day rotation period or the single solar cycle. Examples when such other variations have been neglected are the following:

1. Isolated measurements taken over periods spanning several years have been compared when some solar index, like the 10 cm radio flux or sunspot number, has a small range. Then the differences have been interpreted as indicating experimental errors, rather than true solar UV variations.
2. A group of separate measurements over about a four-year period were averaged to obtain an average sunspot minimum flux.

3. Satellite measurements were adjusted in absolute magnitude so that their initial measurements were consistent with rocket flight measurements recorded as much as a year prior to the satellite measurements using solar activity indices like the 10.7 cm solar radio flux or sunspot number to judge the relative levels of solar UV activity.

These recent practices are dangerous and should be avoided because they neglect the possibility of long-term secular trends and assume that solar indices accurately scale the UV flux levels between two or more particular days.

DOUBLE-SUNSPOT CYCLE

Considering our lack of knowledge of the UV variability over the single solar cycle, it is clear that we do not know much about the UV variations related to the 22-year double solar cycle, i.e., the solar magnetic polarity cycle. On the other hand, a search for such variations is important because of studies suggesting atmospheric variations with periods of the order of 20 years are linked with solar activity (Herman and Goldberg, 1978). We would like to point out the old result that odd numbered solar cycles are statistically related in intensity and temporal structure to their preceding even cycles, where the peak smoothed sunspot number of odd cycles is larger than their preceding even cycle (Vitinskii, 1965, pp 24-26). Such a pairing of cycles suggests that solar electromagnetic radiation may have a double cycle dependence.

SECULAR TRENDS AND LONG-TERM CYCLIC VARIATIONS

Heath (1980) has presented evidence that suggests a secular decrease in solar UV flux from the peak of the solar cycle 20 to near the peak of cycle 21, particularly at wavelengths below 300 nm, with the strongest decrease near 210 nm, and the effect being overcome by solar cycle variations below 200 nm. Accurate future measurements are needed to confirm such a trend. In the meantime, we should not analyze data in ways that assume such secular trends do not exist, as discussed above.

Figure 9 shows evidence presented by Heath (1980) suggesting a long-term variation possibly related to the Gleissberg ninety year cycle. Considering the sources of errors suggested by recent satellite and independent concurrent measurements, the error bars in Figure 9 may be optimistic. For confirmation, overlapping or occasionally concurrent measurements are needed. Figure 10 shows a comparison of faculae area A_F data with sunspot area A_S and sunspot number R. The important thing is that in A_F a cycle of about 44 years seems more evident than a 90 year cycle. Consequently, as we search for long-term trends in future data, we might find long-term periodicities other than those evident in the sunspot numbers. (The possible 90-year period in R is better evident in figures spanning about two hundred years.) Note in the cases of R and A_S in Figure 10 that the intensities peak higher for odd numbered cycles than for their preceding even numbered cycles, but a similar systematic relation is not evident for A_F.

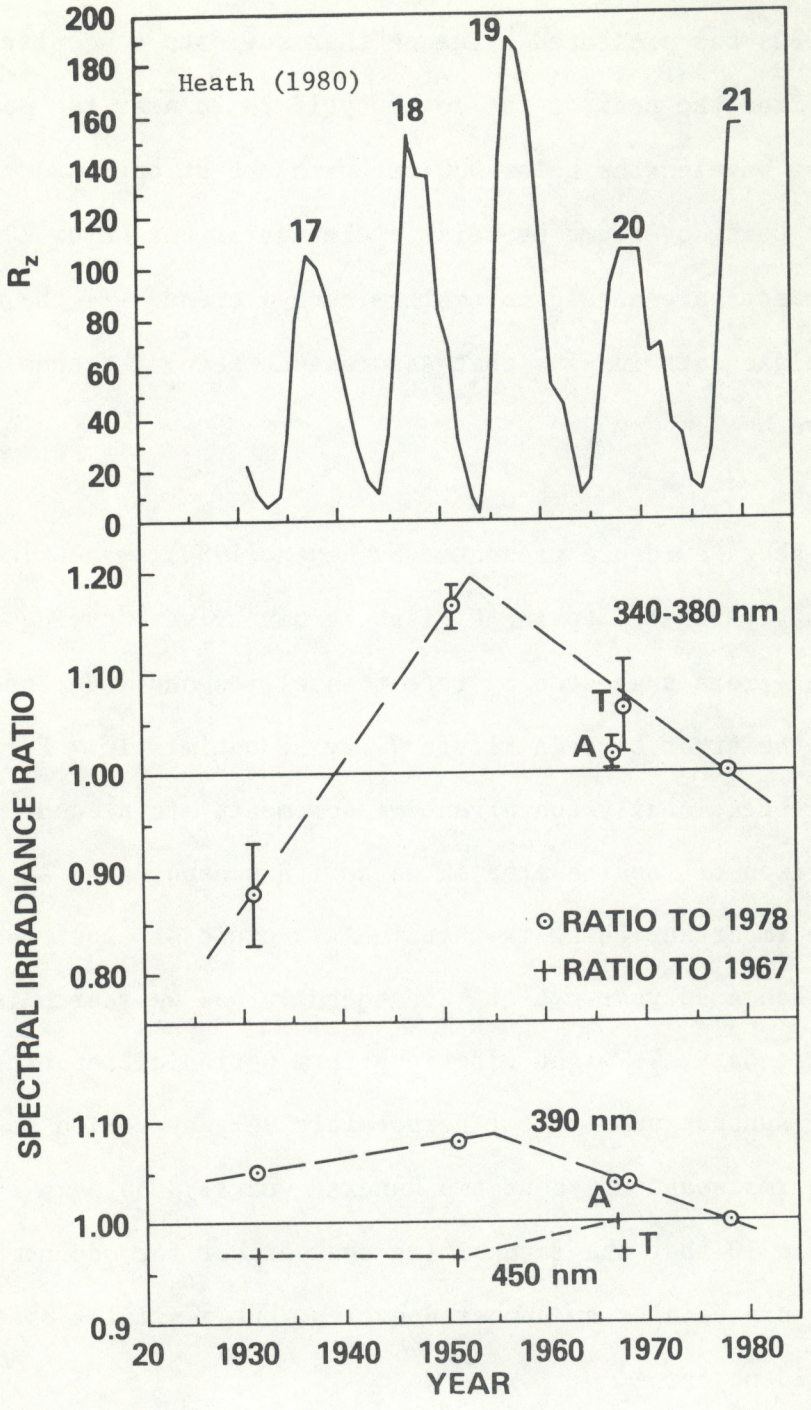

Figure 9.--Long-term variations.

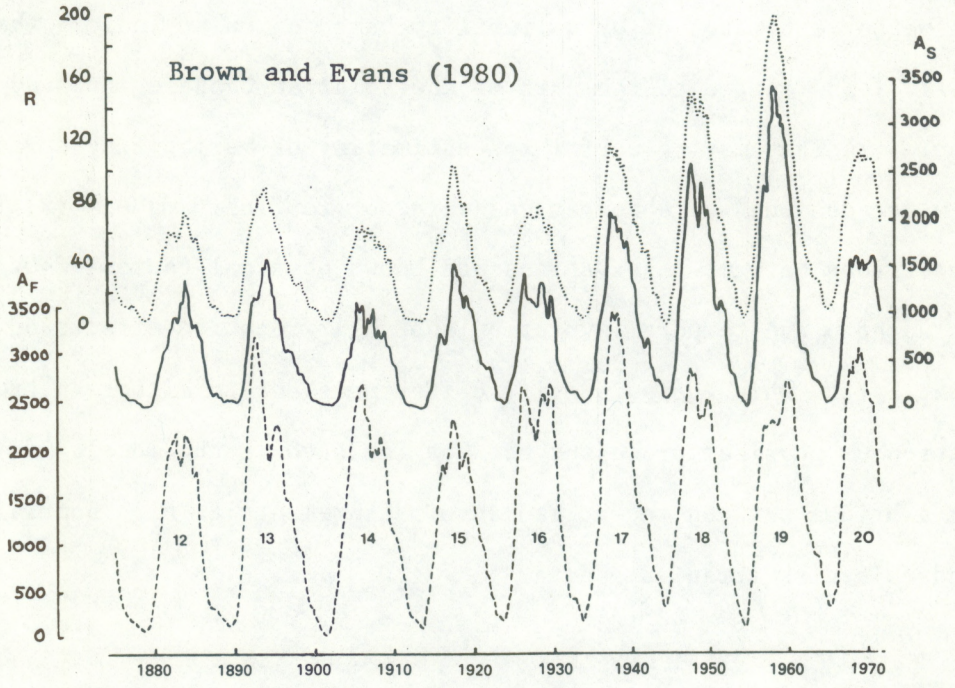

Figure 10.--Differences in long-term trends of solar faculae relative to the trends in sunspot number or sunspot area.

MODELING SOLAR UV VARIABILITY

Recently, models of the temporal variations of solar UV flux have been developed by Lean et al. (1982) and Oster et al. (1982) using ground-based Ca K line observations of plages to empirically estimate the UV flux variations from these same active regions.

These models are important for the following reasons: (1) They should provide better estimates of UV variability based on solar indices that are physically less related to the part of the solar atmosphere involved in the UV emission. (2) They may be useful for estimating UV variability during the past few decades when UV observations were not routinely made. (3) They permit comparisons between observations and known physical causes of UV variability including plage temporal evolution and solar rotation effects on viewing plages at Earth, which help identify differences due to either instrument degradation or physical processes not yet included in the model. (4) They can provide a bridge between recent radiance measurements at high spatial resolution and full-disk irradiance data.

Figure 11 shows the principle behind such models. The Lyman α photo was taken from a rocket above the Earth's atmosphere while the Ca K photo was taken at a mountaintop observatory. Lyman α is emitted from the very top of the solar chromosphere, near the base of the tenuous chromosphere-corona transition region, while the Ca K line core is emitted near the middle of the chromosphere. The detailed spatial structures of these two different emissions are quite similar, especially for the large bright splotches called plages. The

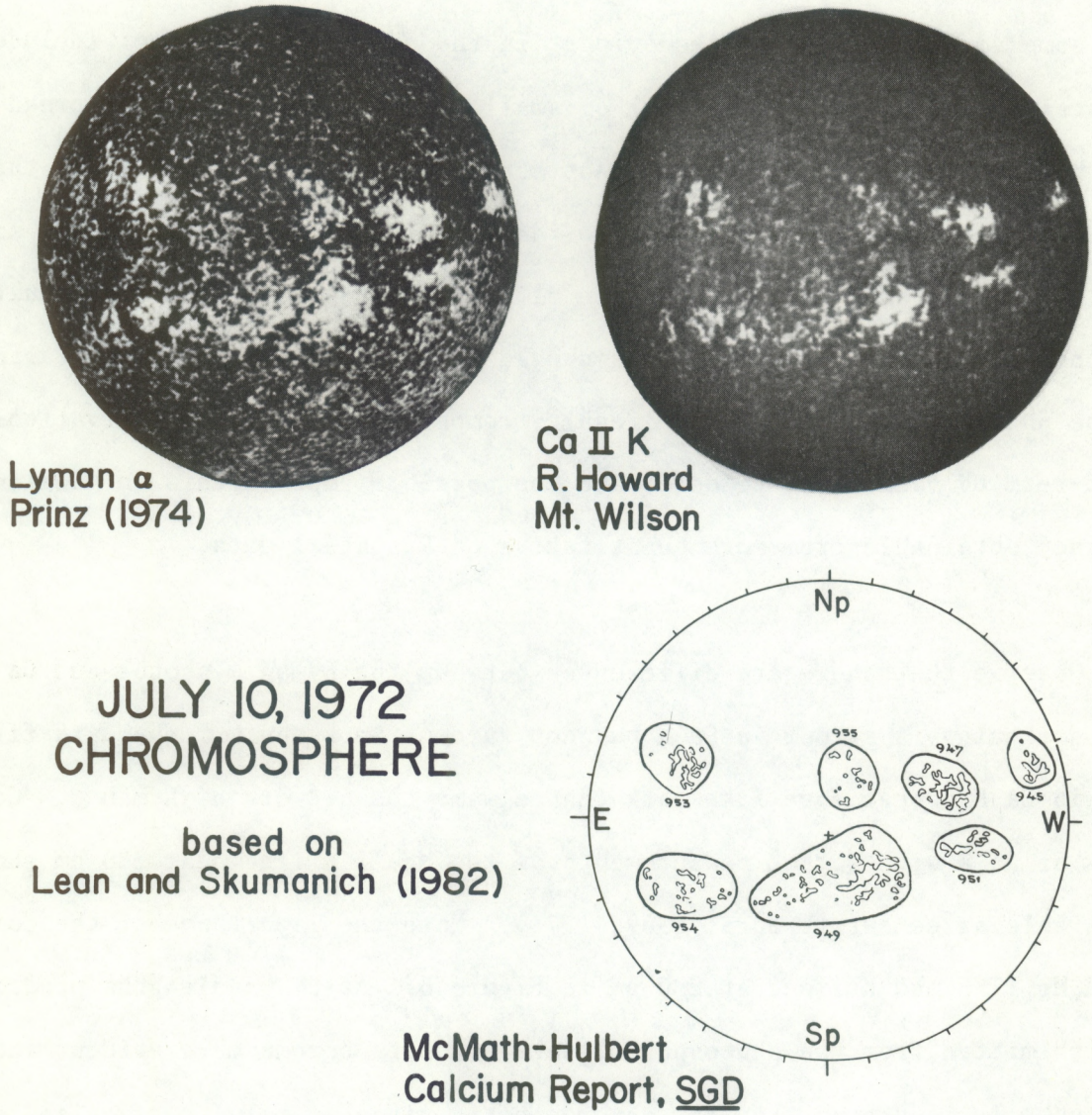

Figure 11.--Comparison of solar spatial structure observed in Lyman α, Ca II K line and the plage scalings used to determine the standard tabulations of plage location and area.

figure in the lower right illustrates the active regions (encircled and numbered) that were scaled for standard daily solar activity reports, which include the solar location, total plage area, and an observer's qualitative estimate of the brightness of the brightest patch in a plage group. Notice that some small or faint plages evident in the photographs are not included in the scalings. Observe the network of small bright cell boundaries spread over the whole sun. Dark filaments are not scaled. The current models use the standard calcium reports. The loss of data from the photographs to the simple scalings is probably the major source of error in the current model results. The photographs still exist. Tests should be run using photometric scalings of the photographic data and the results compared with recent observations of short-term UV variations to determine the possible improvements in modeling accuracy obtainable from more quantitative Ca K spatial data.

Observe that there are differences between the Lyman α photos and Ca K. Limb darkening is strong in Ca K but not evident in Lyman α. The dark filaments seen in Ca K appear more like dark channels in the network of Lyman α. Comparisons of Ca K with rocket measurements of the Mg II K line near 280 nm show comparable agreement (Fredga, 1969, 1971). Note the importance of the combined Mg II H and K lines at 280 nm in Figure 6. At UV wavelengths predominantly emitted from the photosphere, dark sunspots become more evident and the photospheric counterpart of the chromospheric plage, namely the faculae, and the photospheric network are more tenuous (Bonnet, 160 nm solar photographs, private communication). These differences are accounted for in Lean's UV/Ca-K model at different UV wavelengths by correcting for the solar location of a plage and using center-to-limb observations of Samain (1979). The absolute intensity was adjusted to be consistent with that of Brasseur and Simon (1981).

Figure 12 shows an example of the Lean/NOAA-UV81 Model (Lean et al., 1981, 1982). It includes three components, the quiet sun, the active network (and plagettes) and the plage component. The latter component is modeled from the Ca K plage data. The active-network term is assumed to be uniform in solar longitude and produced from the remnants of former active regions.

The brightness of the active network is smaller than in bright plages and the area of individual patches of active network is quite small. On the other hand, the number of such elements is large so that the total area of the active network is significant and the magnitude of the active-network term is quite large. The quiet sun here means the dark cell centers and invariant portion of the network and is assumed to be constant with time at least during one cycle. The time dependence of the active network term is not yet well determined. In this model it was estimated from the total plage area smoothed over--seven solar rotations and lagged by one solar rotation. This lag assumes that the amount of plage remnants that contribute to the active network and plagettes on a given day is related to a smoothed estimate of plages one rotation ago. Further uncertainties in the model are the active-network contrast and center-to-limb dependences as functions of wavelength. Because the active network term is so large, it is important that further research be aimed at better refining this term.

Note in Figure 12 that there are four peaks in UV activity in 1979 and 1980, similar to Heath's semiannual variation discussed earlier. Note also that the active-network term tends to broaden the temporal half width of the UV enhancements associated with major rounds of solar activity. If the active network or associated effects also contribute to UV enhancements at wavelengths

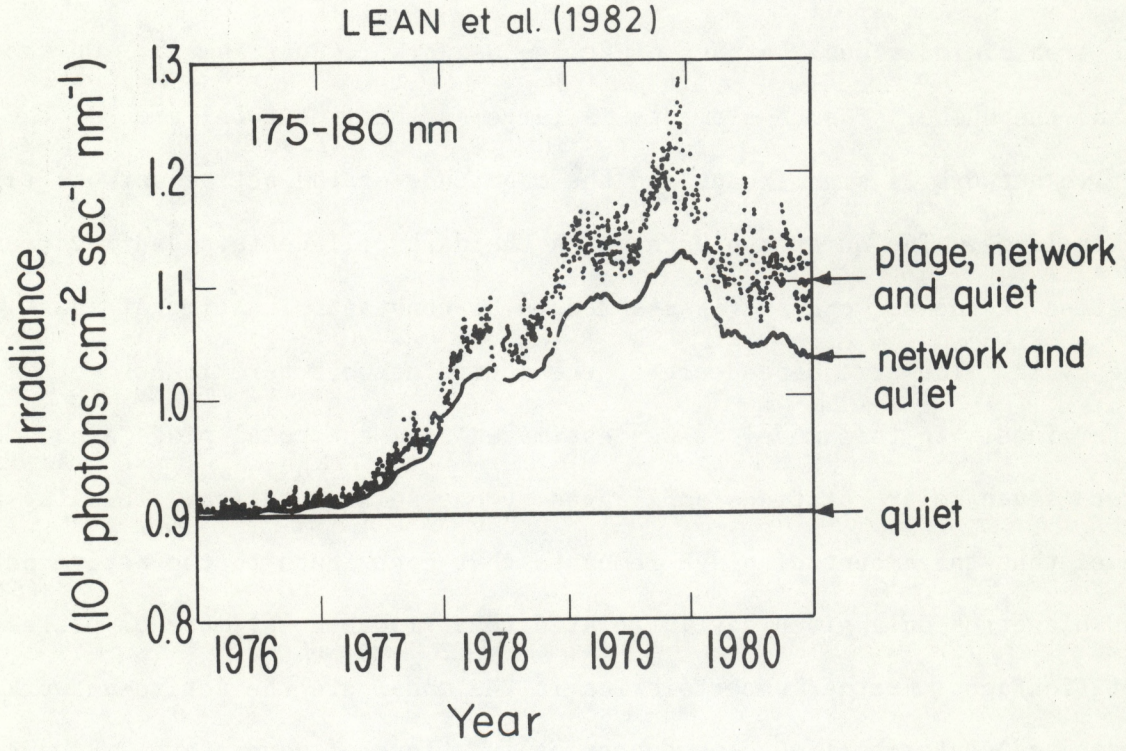

Figure 12.--Modeled UV flux from the minimum through the peak of solar cycle 21.

longer than 300 nm, it may explain the quasi-semiannual variation. If true, then Figure 12 suggests the effect is not semiannual in general since the corresponding structure in Figure 12 in 1977 and 1978 is closer to an annual variation.

Figure 13 shows the results for the Lean/NOAA-UV82 model (Lean and Skumanich, 1982) which is like the 81 model but adapted to Lyman α data. At this wavelength, the plage and active-network components are comparable in magnitude while in Figure 12 the active-network term was more than twice as large as the plage component.

Furthermore, if the active-network term contributes to Heath's 300-400 nm quasi-semiannual variation discussed earlier, and if this is some of the "missing" energy flow blocked in the total solar irradiance by dark sunspots, then the temporal evolution of this active-network component may not simply be caused by decaying remnants of old active regions. Clearly, further research is needed to define the relative strength and temporal variation of the active-network term.

Most experimenters involved in measuring the solar UV spectral irradiance do not yet consider models of the UV flux to be very worthwhile because of the uncertainties in some of the quantities used in the models and because entire physical processes that cause variations in their measurements may not be included in the models. Models need verification from independent measurements and should be considered equally suspect as the measurements of long-term trends because of the uncertainties caused by instrument degradation problems.

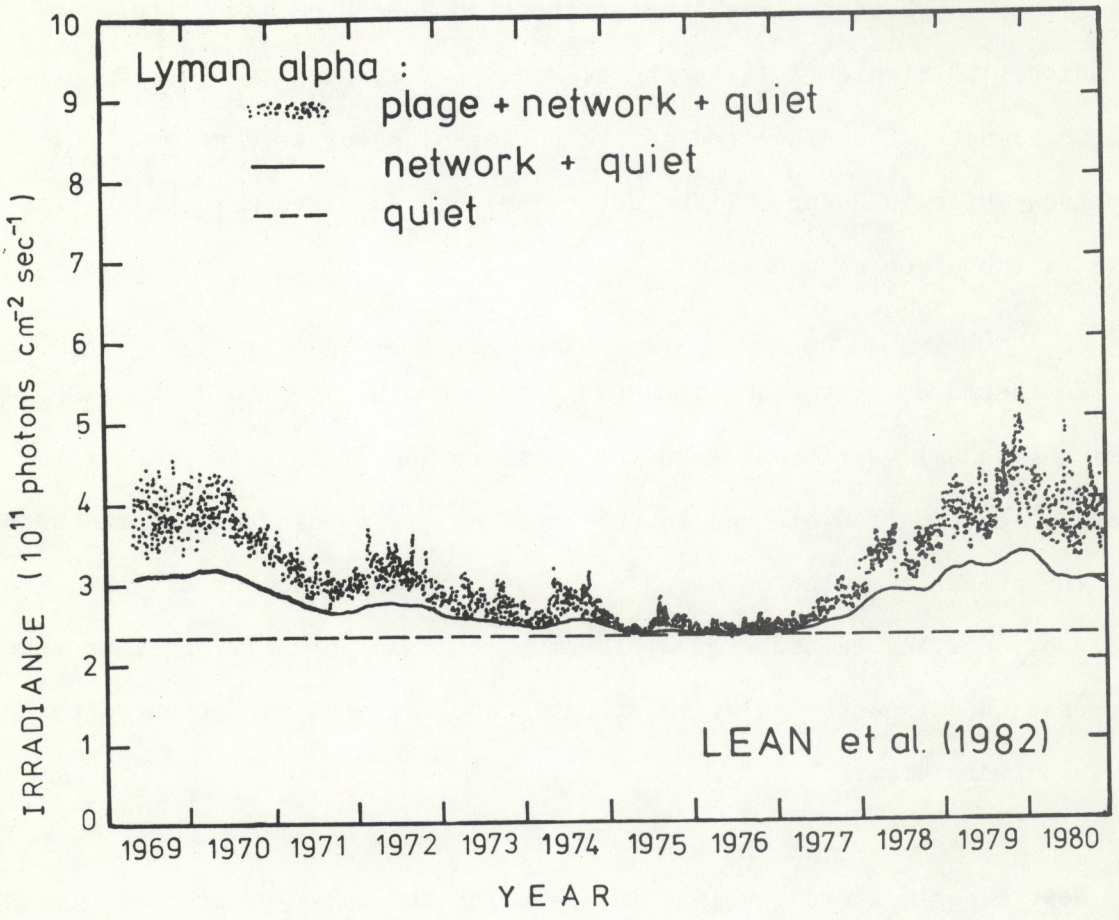

Figure 13.--Modeled Lyman α flux from the peak of solar cycle 20 through the peak of cycle 21.

Figure 14 compares the model results for Lyman α with the observations previously discussed in Figure 8. Note that the model exceeds the observations in 1969 and falls below the observations from 1976-1980. Lean et al. (1982) have pointed out that Hinteregger's EUV minimum in April 1975 was a short-term local minimum followed by a long lasting minimum in 1976, the period of sunspot minimum. There is no evidence in the model for a rise in UV flux until 1977. Therefore, either there is some unknown physical process missing in the model for 1976 or there is an unknown error in the combination of the rocket flight measurements in 1976 and the setting of the absolute value of the satellite measurements starting in 1977. The temporal variations of the model agree well with the OSO-5 results. The model exceeds these observations in 1969 and 1970, but they nevertheless agree within the measurement uncertainty of 40%. Note there is no jump in the model in December, 1979, as seen in the AE-E satellite data.

Figure 15 compares the short-term variations from the Lean/NOAA-UV82 model with the AE-E satellite and with three other estimates based on solar-index algorithms. Each of the four pairs of curves are adjusted to provide good fits in June and July, 1979. The Bossy and Nicolet results were derived from these AE-E observations, but greatly overestimate the enhancement of November 10, 1979 and greatly underestimate the AE-E observations during the enhancement of December 15, 1979. Such problems are probably caused by physical processes involved in the 10.7 cm solar radio flux that are only weakly related with the physical processes causing the Lyman α variations. Problems with using daily solar indices to estimate UV fluxes are discussed in the next section. Both the estimates of Cook et al. and Vidal-Madjar are based on the

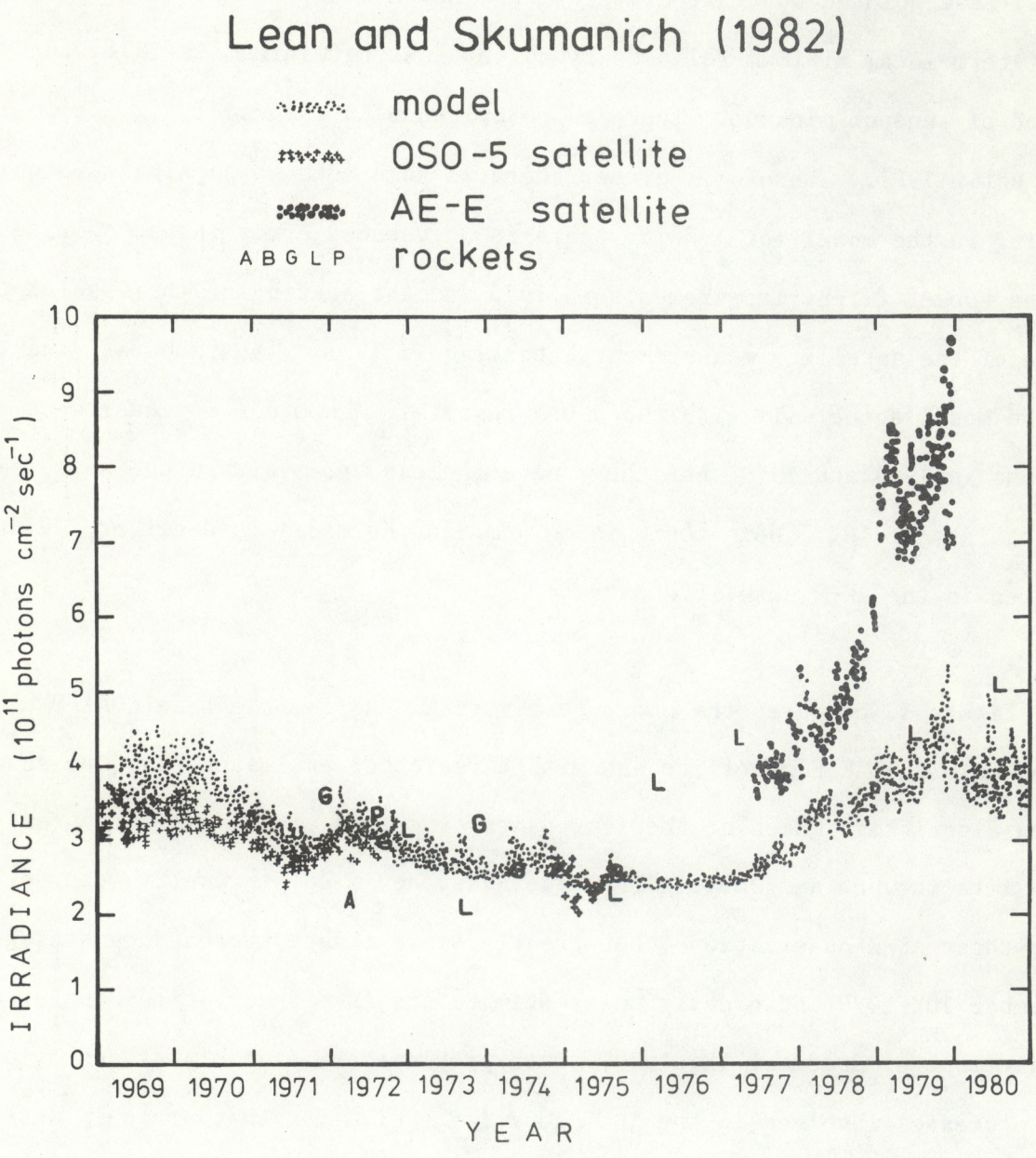

Figure 14.--Comparison of Lean's model with the observations in Figure 8 for Lyman α.

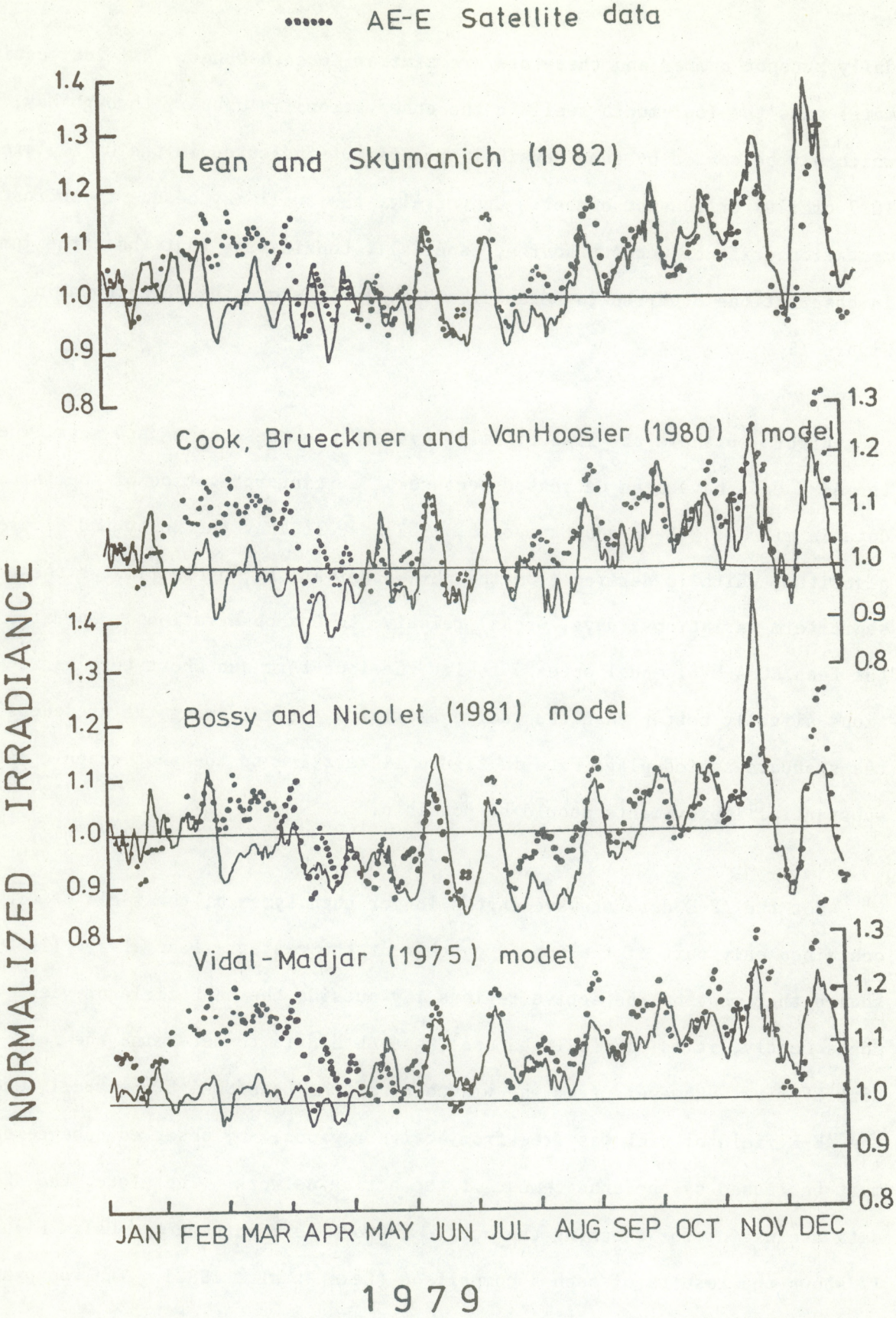

Figure 15.--Comparison of model results with Hinteregger's (1981) AE-E observations for short-term Lyman α variations.

daily sunspot number and therefore are similar to each other. All four estimates miss the four-month swell in the observations in January through May, which may be caused by some physical process not indicated in the Ca K plages, 10.7 cm flux or sunspot number. Conversely, the swell may be due to an instrumentation drift of unknown source, especially considering that the large jump in observations occurred in December, 1978, just before the data shown in Figure 15.

Figure 16 shows the rise of solar cycle 21 in these same data sets, where the AE-E data have been decreased because of a reinterpretation of the initial data in mid 1977 (Lean and Skumanich, 1982). Note that the Bossy and Nicolet algorithm, which is derived from the AE-E observations, overestimates the short-term variations (days, weeks) relative to the observations. Overall, the Lean/NOAA-UV81 model appears to fit the long-term and short-term variations slightly better than the indice estimates. Considering the crudeness of the standard scaled plage data in Figure 11 relative to the photographic data, substantial improvements should be possible.

For the AE-E data at wavelengths longer than Lyman α, the field of view contained only part of the sun, a patch near the center. Lean et al. (1982) showed that most of the active regions lay outside the AE-E field of view. Consequently, it is difficult to use these AE-E data to determine the full-disk UV flux. However, from the viewpoint of the Lean/NOAA-UV 81 model, when the AE-E field of view was free from active regions, any observed enhancement must be caused by the enhancement of the active network. Therefore, the AE-E data are useful for checking the active-network term in Lean's model. Figure 17 shows the results of such a comparison (Lean et al., 1982). The top panel

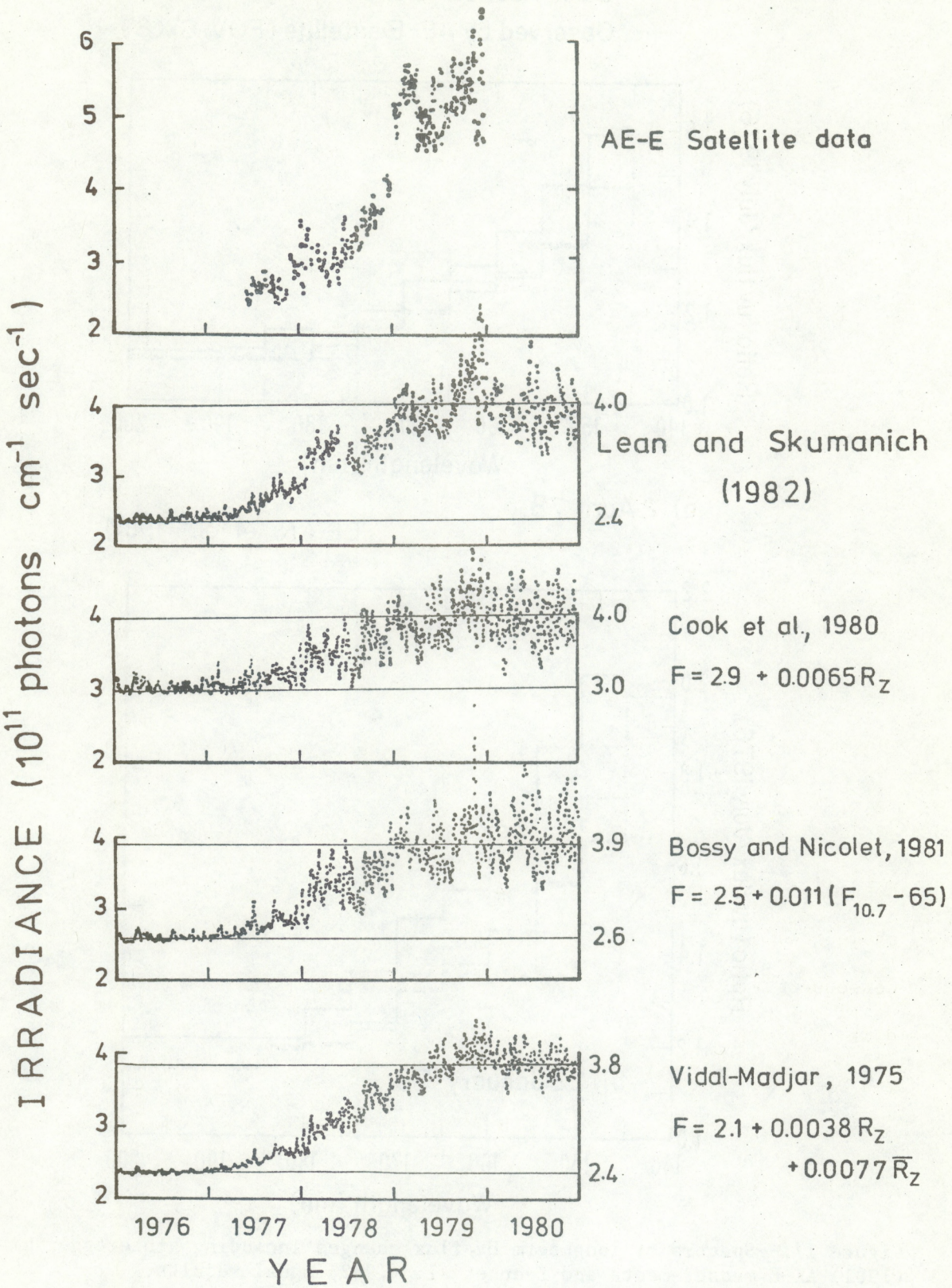

Figure 16.--Comparison of model results with Hinteregger's (1981) AE-E observations for long-term Lyman α variations.

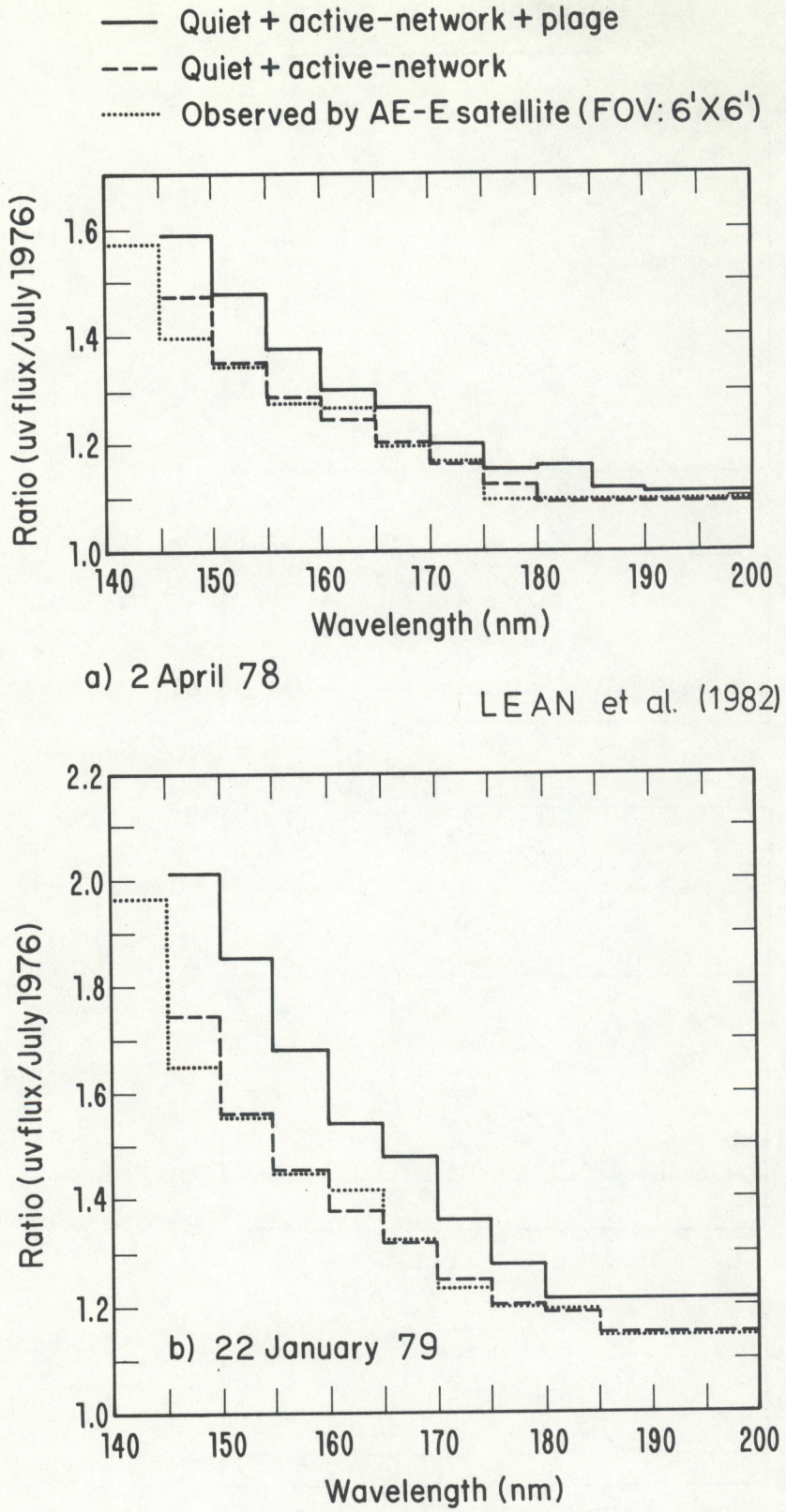

Figure 17.--Spectra of long-term UV flux changes including Hinteregger's (1981) AE-E measurements and Lean et al. (1982) model results.

corresponds to a time about midway up the rise of solar cycle 21 while the bottom panel is early in the year of the maximum of the cycle. On April 2, 1978, the AE-E field of view was free of active regions; and on January 22, 1979, there were minor portions of plages within the field of view. July 1976, was used in the flux ratios as being representative of sunspot minimum conditions. The dashed curve represents the ratio of the active-network plus quiet sun components to the quiet-sun component of the full-disk model calculations excluding the plage contribution. These results match the dotted histogram results for the AE-E observations quite well. Furthermore, the solid-line histogram represents the model calculations including the plages. The amount this curve exceeds the AE-E results estimates the amount of variability not evident in the AE-E data due to the limited field of view and the presence of many plages outside the field of view. In conclusion, the AE-E observations are consistent with the model's active network term, a very important corroboration.

SOLAR ACTIVITY INDICES

The sunspot number and 10.7 cm solar radio flux are useful as a general guide to the level of solar activity. However, they are not precise indicators of the solar UV flux. They can give very erroneous UV estimates when they are used for particular days rather than for average effects. An example of this is when rocket flight data recorded months before a set of satellite data are used to adjust the absolute value of the satellite measurements. The satellite raw observations on a day with nearly the same value of solar index as that of the date of the rocket flight measurements are compared with the rocket measurements and revisions are thereby derived. Hopefully the comments

below will stop this practice and emphasize the need for concurrent measurement.

The slowly-varying component of the 10.7 cm radio flux is emitted from the active region corona, not from the chromosphere, and involves several different emission mechanisms. Figure 7 shows that the 10.7 cm radio flux from an active region near and beyond the limb of the sun greatly exceeds its UV flux near 200 nm relative to when the region is near the center of the disk. Consequently, whenever strong regions at large solar central-meridian-distance (CMD) contribute greatly to the 10.7 cm radio flux, the latter overestimates the UV flux relative to when the dominant regions are near the center of the disk. Part of the 10.7 cm radio flux is emitted by gyroresonance absorption and is sensitive to the strength of the magnetic field so that active regions with strong magnetic fields may emit 10.7 cm radio flux more strongly than older spotless regions. Many active regions with plages have no sunspots or very minor spots (Puga and Donnelly, 1982). Donnelly et al. (1982) showed that the regions with large dark sunspots that cause the large dips in total solar irradiance produce only medium, not outstanding, UV enhancements. Although the daily 10.7 cm measurement is corrected for impulsive radio bursts, many gradual rise and fall events may contaminate slightly the 10.7 cm data because they are too small to identify as distinct flare enhancements. In a comparison of concurrent solar soft X-ray data with 10.7 cm radio data, where data complicated by flares were eliminated, most of the eliminated cases were cases where the daily 10.7 cm radio flux did not indicate a flare correction but the X-ray data showed the presence of a flare (Donnelly, 1982). Even when corrections are made for impulsive radio bursts, the corrected value may still be contaminated by undetected gradual flare enhancement. These effects can

cause two days to have similar 10.7 cm radio fluxes and yet have quite different UV fluxes. These effects probably contribute to the large errors in Bossy and Nicolet's overestimate of Lyman α on November 10 and underestimate on December 12, 1979, in Figure 15. Solar Geophysical Data (SGD) shows that on November 10 several regions with strong sunspots were present, including regions at large CMD, and few plages were from spotless active regions. GOES soft X-ray data in SGD show that numerous flares occurred and that it would be very difficult to obtain data unaffected by the decay of the thermal coronal flare enhancement. Similar circumstances occurred throughout the November 6-14 peak in daily 10.7 cm radio flux. During the following solar rotation, for example on December 12, the sunspots had decayed greatly and mainly weak spot groups remained. Numerous spotless plages were present. Soft X-ray data suggest that a good estimate of the quiet background could be obtained just before and at 1700 UT (noon in Ottawa) just before the fast flare of about 1710 UT, December 12, 1979. Consequently, there are clear physical explanations for why the Ca K plage-based Lean/NOAA-UV82 model should closely fit these two peaks, while the 10.7 cm radio flux greatly overestimates one and underestimates the other.

The 10.7 cm radio flux and sunspot number are of course correlated with the solar UV flux because all three are generally related to the number and size of active regions. The more smoothing applied to the data, the higher the correlation because the differences due to CMD and magnetic field orientation and strength distribution among active regions become smoothed out to average values.

Sunspot numbers give no weight to spotless plages and very little to plages with isolated spots. That is why the UV estimates of both Cook et al. (1980) and Vidal-Madjar (1975) underestimate the UV peak of December 12, 1979, in Figure 15, while Lean's Ca K plage model fits it well. The sunspot number also weights those active regions with several small sunspots equally with regions having the same number of large spots. Furthermore, regions on the visible disk but near the limb have similar weight to regions at the center of the disk, unlike the UV dependence on CMD in Figure 7. For example, on both October 17, 1976, and March 16, 1980, the daily sunspot number was 36 (SGD). The Ca K daily plage index was 13.5 for the first day and 42.8 for the second. Certainly not comparable days. Note that Lean's model in Figures 12 and 13 based on Ca K plage data similarly finds these two days to be quite different, including a large difference in the active network component.

SOLAR SOFT X RAYS

Solar soft X rays affect the D-region of the ionosphere and upper mesosphere when the 1-8A flux above the Earth's atmosphere exceeds about 10^{-6} Wm^{-2}. This threshold level occurs because it is the level where the soft X-ray photoionization rate begins to be comparable with that of Lyman α in the upper D-region and cosmic rays in the low D-region. Kreplin et al. (1977) review solar soft X-ray variability through 1975.

Solar 1-8A soft X-rays have been monitored since July, 1974, by the SMS and GOES satellites. Daily graphs of these data have been published in Solar Geophysical Data starting with the data of September, 1978. Donnelly (1981)

and Donnelly and Bouwer (1981) provide daily graphs from July 1, 1974 through August, 1978, and graphs of major flares through December, 1980. Bouwer et al. (1982b) provide tables of daily means, which are sometimes dominated by large solar flares, and a daily estimate of the nonflare background X-ray flux for 1977-1981. Puga and Donnelly (1982) include tables for 1975-1976. The analysis of quasistationary epochs and their relation to other solar measurements of large-scale solar structure are presented by Bouwer et al. (1982a).

Because of the strong influence on D-region ionization during years near sunspot maximum and during solar flares and because of their very large variability, solar soft X-rays should be considered as one of the sources of solar-induced variability in the geomagnetic field in the studies of the possible coupling of geomagnetic activity into the lower atmosphere. However, as far as soft X-rays affecting the neutral atmosphere, they are much less important than Lyman α in the mesosphere and the 175-205 and 205-295 nm bands in the stratosphere.

FUTURE MEASUREMENTS

Figure 18 shows recent measurements and the current plans for future measurements in the UV wavelength range based on Vostreys and Malitson (1981). Hopefully the NIMBUS-7 and SME measurements will last long enough to overlap with the future SBUV/2 instruments that are currently being built to fly on future NOAA satellites. The important features are a nearly continuous series of satellite measurements with concurrent ground-based measurements at wavelengths longer than 300 nm. Furthermore, a series of rocket-flight measurements and a new generation of UV spectroradiometers for shuttle flights should

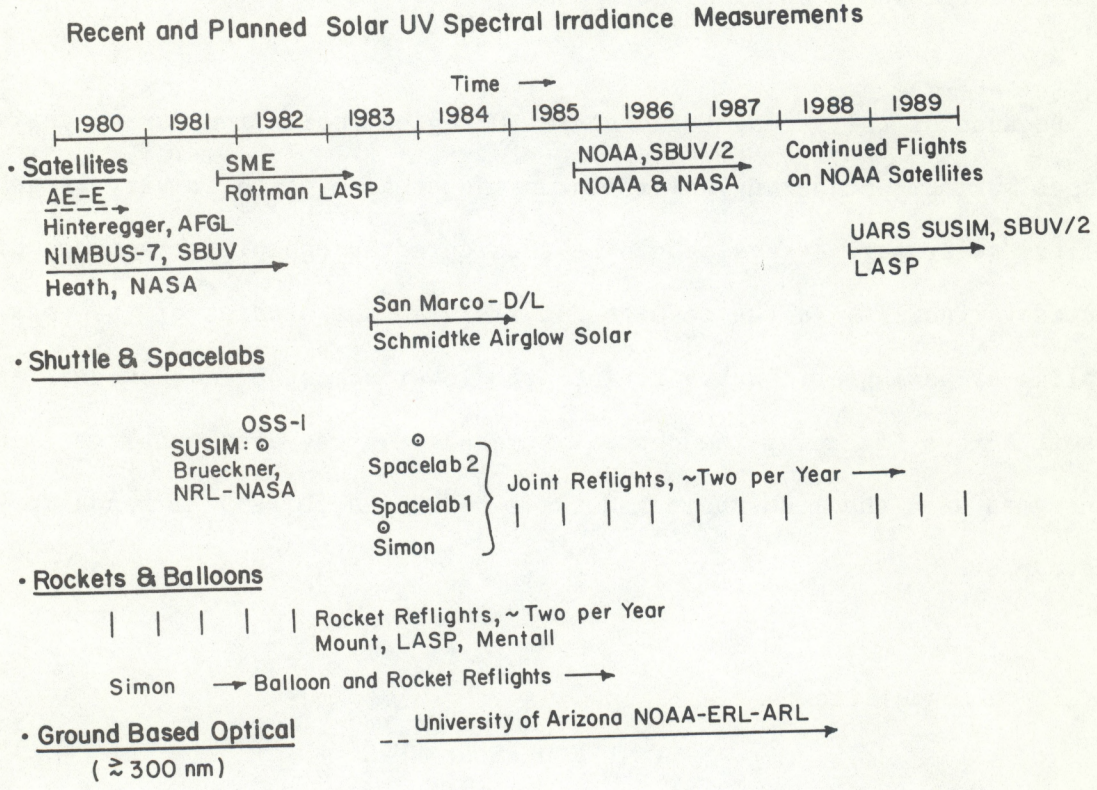

Figure 18.--Recent and planned solar UV spectral irradiance measurements.

provide the needed re-calibration of the satellites. The satellites will then provide the measurements of short-term variations needed to interpret each rocket or shuttle measurement in order to accurately determine long-term trends. Note that the observed approximately semiannual variations discussed previously suggest that an even spacing of two calibration flights per year may be an inappropriate choice. The observed quasi-semiannual variations did extend into the 300-400 nm range. Consequently, the ground-based measurements should provide an important check at least for the longer wavelengths.

Note that the plans include concurrent cross-checks and recalibrations. The new generation instruments include on-board calibrations and some optical elements that are only occasionally deployed to test the deterioration of the corresponding elements that are frequently deployed.

CONCLUSIONS

1. Recent satellite measurements have accurately measured short-term variations over days, weeks and months in the 175-205 nm range pertinent to stratospheric O_3 production and in the 205-295 nm range that heats the stratosphere and photodissociates O_3. See Figures 2-6.

2. Important UV enhancements lasting several months, including enhancements of 1 to 3% in the 300-400 nm range, have been observed by Heath (1982). They appear to be related to major rounds of solar activity and occur nearly semiannually in 1979 and 1980. Corroborating observations and a better physical understanding of this phenomena is needed. Heath (1982)

has suggested these enhancements may be part of the missing solar energy blocked in the total solar irradiance by dark sunspots.

3. Measurements of UV variations over a solar cycle are inadequate. Model estimates are available.

4. Models of solar UV flux variations based on Ca K plage data currently estimate short-term and long-term UV variations better than solar indices like the daily 10.7 cm solar radio flux and sunspot number. The latter indices physically are less closely related to the active region plages, faculae and active network that dominate UV flux variations. Considerable improvement in UV model estimates may soon be achieved by using more quantitative Ca K data than the standard plage scalings.

5. Secular changes and long-term periods (decades) in UV variability have been suggested. The evidence is insufficient and better measurements of their characteristics are needed. In the meantime, current practices in analyzing UV data that assume such trends do not exist should cease.

ACKNOWLEDGMENTS

I thank Don Heath of NASA GSFC for use of his prepublication results presented at the Fifth International Symposium on Solar-Terrestrial Physics held in Ottawa, May 17-22, 1982. I also benefited greatly from preprint results and discussions with Dave Bouwer and Judith Lean, both of CIRES, University of Colorado, Boulder, Colorado. I thank Jim Heyser and Larry Puga for their help in analyzing data.

REFERENCES

Ackerman, M. and P. Simon, Rocket measurement of solar fluxes at 1216Å, 1450Å and 1710Å, Solar Phys., 30, 345-350, 1973.

Bossy, L. and M. Nicolet, On the variability of Lyman-alpha with solar activity, Planet. Space Sci., 29, 907-914, 1981.

Bouwer, S. D., D. F. Heath and P. S. McIntosh, Solar variability during several years of solar cycle 21 at coronal, chromospheric and photospheric wavelengths, Paper STP I. 4.1, Fifth International Symposium on Solar-Terrestrial Physics, Ottawa, Canada, May 17-22, 1982a.

Bouwer, S. D., R. F. Donnelly, J. Falcon, A. Quintana, G. Caldwell, A Summary of Solar 1-8A Measurements from the SMS and GOES Satellites, 1977-1981, NOAA Tech. Memo. ERL 999 - SEL 99, NOAA/ERL Boulder, Colorado 80303, 88 pp., 1982b.

Brasseur, G. , and P.C. Simon, "Stratospheric chemical and thermal response to long-term variability in solar UV irradiance," J. Geophys. Res., 86, 7343-7362, 1981.

Brown, G. M., and D. R. Evans, The use of solar faculae in studies of the sunspot cycle, Solar Phys., 66, 233-243, 1980.

Brueckner, G. E., J. -D. F. Bartoe, O. Kjeldseth Moe, and M. E. Vanhoosier, Absolute solar ultraviolet intensities and their variations with solar activity. I. The wavelength region 1750 - 2100 A, Astrophys. J., 209, 935-944, 1976.

Bruner, E.C., Jr., private communication reported by Vidal-Madjar (1977).

Cook, J. W., G. E. Brueckner and M. E. VanHoosier, Variability of the solar flux in the far ultraviolet 1175-2100Å, J. Geophys. Res., 85, 2257-2268, 1980.

Donnelly, R. F., Comparison of nonflare solar soft X-ray flux with 10.7 cm radio flux, accepted for publication in J. Geophys. Res., 1982.

Donnelly, R. F., SMS-GOES Solar Soft X-Ray Measurements, Part I. SMS-1, SMS-2 and GOES-1 Measurements from July 1, 1974, through December 31, 1976, NOAA Tech Memorandum ERL SEL-56, Space Environment Lab., NOAA ERL, Boulder, CO. 80303, 201 pp, 1981.

Donnelly, R. F., and S. D. Bouwer, SMS-GOES Solar Soft X-Ray Measurements, Part II. SMS-2, GOES-1, GOES-2 and GOES-3 Measurements from January 1, 1977, through December 31, 1980, NOAA Tech Memorandum ERL SEL-57, Space Environment Lab., NOAA ERL, Boulder, CO. 80303, 206 pp, 1981.

Donnelly, R. F., D. F. Heath and J. L. Lean, Short-term variations in solar UV spectral irradiance, total solar irradiance and soft X-rays, submitted for publication in J. Geophys. Res., 1982.

Fredga, K., Spectroheliograms in the Mg II line at 2795.5Å. Solar Phys., 9, 358-371, 1969.

Fredga, K., A comparison between Mg II and Ca II spectroheliograms, Solar Phys., 21, 60-81, 1971.

Heath, D. F., Possible responses of the middle and upper atmosphere to variations in solar output, Fifth International Symposium on Solar-Terrestrial Physics, held May 17-22, 1982, Ottawa, Canada, to be published in the conference proceedings, 1982.

Heath, D. F., A review of observational evidence for short and long term ultraviolet flux variability of the sun, Sun and Climate, Centre National D'Etudes Spatiales, 18 Avenue Edouard - Belin, 31055 Tolouse Cedex, France, 447-471, 1980.

Heath, D. F., Space observations of the variability of solar irradiance in the near and far ultraviolet, J. Geophys. Res., 78, 2779-2792, 1973.

Heath, D. F. and H. Park, NIMBUS-7 SBUV observations of solar UV spectral irradiance, to be submitted to J. Geophys. Res., 1982.

Herman, J. R., and R. A. Goldberg, Sun, Weather and Climate, NASA SP-426, Superintendent of Documents, Stock No. 033-000-00747-7, U.S. Government Print. Office, Washington, D.C. 20402, 360 pp. 1978.

Heroux, L., and J. E. Higgins, Summary of full-disc solar fluxes between 250 and 1940Å, J. Geophys. Res., 82, 3307-3310, 1977.

Hickey, J. R., L. L. Stowe, H. Jacobowitz, P. Pellegrino, R. H. Maschoff, F. House and T. H. Vonder Haar, Initial Solar Irradiance Determinations from NIMBUS 7 Cavity Radiometer Measurements, Science, 208, 281-3, 1980.

Hinteregger, H. E., Representations of solar EUV fluxes for aeronomical applications, Adv. Space Res., Vol. 1, The Mesosphere and Therosphere, ed. G. Schmidtke and K.S.W. Champion, Pergamon Press, New York, 39-52, 1981.

Hinteregger, H. E., O. E. Bedo, J. E. Manson and D. R. Skillman, EUV flux variations with solar rotation observed during 1974-1976 from the AE-C satellite, Space Res., XVII, 533-544, 1977.

Hinteregger, H. E., K. Fukui and B. R. Gilson, Observational, reference and model data on solar EUV, from measurements on AE-E, Geophys. Res. Letters, 8, 1147-1150, 1981.

Hoyt, D. V. and J. A. Eddy, An Atlas of Variations in the Solar Constant Caused by Sunspot Blocking and Facular Emissions from 1874 to 1981, NCAR Tech. Note No. NCAR/TN-194tSTR, 112 pp., 1982.

Kreplin, R. W., K. P. Dere, D. M. Horan and J. F. Meekins, The solar spectrum below 10A, in The Solar Output and Its Variation, ed. O. R. White, Colorado Assoc. Univ. Press, Boulder, Colorado, 287-312, 1977.

Lean, J. L., A. Skumanich, Variability of the Lyman alpha flux with solar activity, submitted to JGR, 1982.

Lean J. L., D. F. Heath, O. R. White, and W. Livingston, Modelling the Variability of the Solar Ultraviolet Flux, (abstract), EOS, 62, 1017, 1981.

Lean J. L., O. R. White, W. C. Livingston, D. F. Heath, R. F. Donnelly and A. Skumanich, A three component model of the variability of the solar ultraviolet flux: 145-200 nm, to be published in J. Geophys. Res., 1982.

Mount, G. H. and G. J. Rottman, "The solar spectral irradiance 1200-3184 A near solar maximum: July 15, 1980, J. Geophys. Res., 86, 9193-8, 1981.

Mount, G. H., G. J. Rottman and J. G. Timothy, The solar spectral irradiance 1200-2550Å at solar maximum, J. Geophys. Res., 85, 4271-4, 1980.

Oster, L., S. Sofia and K. H. Schatten, Modeling of solar irradiance variations in the UV (abstract 37.02), Bulletin of the Amer. Astron. Soc., 13, 877, 1982.

Park, H., D. F. Heath, R. F. Donnelly, Temporal behavior of the UV solar spectral irradiance observed near the solar maximum (abstract), EOS, 62, 1017, 1981.

Prinz, D. K., The spatial distribution of Lyman-α on the sun, Astrophys. J., 187, 369-375, 1974.

Puga, L., and R. F. Donnelly, Studies of Solar Ca K Plages and UV, X-Ray and 10 cm Variations, NOAA Tech. Memo ERL/SEL, NOAA/ERL, Boulder, Colorado 80303, to be published, 1982.

Rottman, G. J., Rocket measurements of the solar spectral irradiance during solar minimum, 1972-1977, J. Geophys. Res., 86, 6697-6705, 1981.

Rottman, G. J., C. A. Barth, R. J. Thomas, G. H. Mount, G. M. Lawrence, D. W. Rusch, R. W. Sanders, G. E. Thomas and J. London, Solar spectral irradiance, 120 to 190 nm, October 13, 1981 - January 3, 1982, Geophys. Res. L., 9, 587-590, 1982.

Samain, D., Solar continuum data on absolute intensities, center to limb variations and Laplace inversion between 1400 and 2100 A, Astron. and Astrophys., 74, 225-228, 1979.

Schatten, K. H., N. Miller, S. Sofia and L. Oster, Solar irradiance modulation by active regions from 1969 through 1980, Geophys. Res. L., 9, 49-51, 1982.

Simon, P. C., Current solar spectral irradiance observations: a review, A Collection of Extended Abstracts Presented at the Symposium on the Solar Constant and the Spectral Distribution of Solar Irradiance, IAMAP Third Scientific Assembly, held August 17-28, 1981, Hamburg, FRG, ed. J. London and C. Frohlich, available from IAMAP Radiation Commission, NCAR, Boulder, Colorado, USA, pp 50-58, 1982.

Simon, P. C., Solar irradiance between 120 and 400 nm and its variations, Solar Phys., 74, 273-291, 1981.

Simon, P. C., R. Pastiels and D. Nevejans, Balloon observations of solar ultraviolet irradiance at solar minimum, Planet. Space Sci., 30, 67-71, 1982b.

Simon, P. C., R. Pastiels, D. Nevejans and D. Gillotay, Balloon observations of solar ultraviolet irradiance during solar cycle 21, Proc. Sympos. on the Solar Constant and the Spectral Distribution of Solar Irradiance (held in Hamburg, FRG, on August 17-18, 1981), to be published, 1982a.

Smith, E. V. P., and D. M. Gottlieb, Solar flux and its variations, Space Sc. Rev., 16, 771-802, 1974.

VanHoosier, M. E., J. -D. F. Bartoe, G. E. Brueckner, D. K. Prinz, and J. W. Cook, A high precision solar ultraviolet spectral irradiance monitor for the wavelength region 120-400 nm, Solar Phys., 74, 521-530, 1981.

Vidal-Madjar, A., Evolution of the solar Lyman alpha flux during four consecutive years, Solar Phys., 40, 69-86, 1975.

Vidal-Madjar, A., The solar spectrum at Lyman-alpha 1216Å, in The Solar Output and Its Variation, (ed.) O. R. White, Colorado Assoc. Univ. Press, Boulder, Colorado, 213-236, 1977.

Vidal-Madjar, A. and B. Phissamay, The solar Lα flux near solar minimum, Solar Phys., 66, 259-271, 1980.

Vitinskii, Yu. I., Solar Activity Forecasting, translated from Russian (Prognozy solnechnoi aktivnosti, Izdatel'stvo Akademii Nauk SSSR, Leningrad, 1962), Israel Prog. Sci. Transl. NASA-TTF-289, pp. 129, 1965.

Vostreys, R. W. and H. H. Malitson, Report on Active and Planned Spacecraft and Experiments, NSSOC/WOC-A-R&S 81-10, National Space Science Data Center, NASA GSFC, Greenbelt, Maryland 20771, 304 pp., 1981.

Willson, R. C., Solar irradiance variations and solar activity, J. Geophys. Res., 87, 4319-4326, 1982.